

AD-A062 711

UNIVERSAL ENERGY SYSTEMS INC DAYTON OHIO

F/G 20/8

ELECTRON TRANSMISSION THROUGH A VIBRATIONALLY EXCITED GAS.(U)

DEC 77 C A DEJOSEPH

F33615-75-C-1082

UNCLASSIFIED

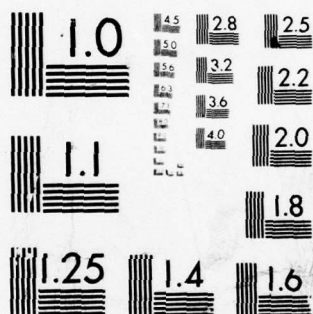
AFAPL-TR-77-82

NL

1 OF 1  
AD  
AD 82711



END  
DATE  
FILMED  
3 --79  
DDC



MICROCOPY RESOLUTION TEST CHART  
NATIONAL BUREAU OF STANDARDS-1963-A

AD A062711

DDC FILE COPY

AFAPL-TR-77-82

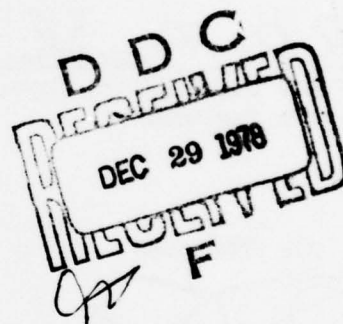
LEVEL

2  
Nul

## ELECTRON TRANSMISSION THROUGH A VIBRATIONALLY EXCITED GAS

CHARLES DEJOSEPH, JR.  
UNIVERSAL ENERGY SYSTEMS, INC.  
3195 PLAINFIELD ROAD  
DAYTON, OHIO 45432

DECEMBER 1977



TECHNICAL REPORT AFAPL-TR-77-82  
Final Report for Period 9 December 1974 - 16 May 1977

Approved for public release; distribution unlimited.

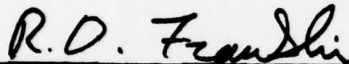
AIR FORCE WRIGHT AERONAUTICAL LABORATORIES  
AIR FORCE SYSTEMS COMMAND  
AIR FORCE AERO PROPULSION LABORATORY  
WRIGHT-PATTERSON AIR FORCE BASE, OHIO 45433

# NOTICE

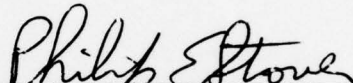
When Government drawings, specifications, or other data are used for any purpose other than in connection with a definitely related Government procurement operation, the United States Government thereby incurs no responsibility nor any obligation whatsoever; and the fact that the government may have formulated, furnished, or in any way supplied the said drawings, specifications, or other data, is not to be regarded by implication or otherwise as in any manner licensing the holder or any other person or corporation, or conveying any rights or permission to manufacture, use, or sell any patented invention that may in any way be related thereto.

This report has been reviewed by the Information Office (OI) and is releasable to the National Technical Information Service (NTIS). At NTIS, it will be available to the general public, including foreign nations.

This technical report has been reviewed and is approved for publication.



RICHARD D. FRANKLIN, Capt, USAF  
Project Engineer



PHILIP E. STOVER  
Chief, High Power Branch

FOR THE COMMANDER



JAMES D. REAMS  
Chief, Aerospace Power Division

"If your address has changed, if you wish to be removed from our mailing list, or if the addressee is no longer employed by your organization please notify AFAPL/POD-2, W-PAFB, OH 45433 to help us maintain a current mailing list".

Copies of this report should not be returned unless return is required by security considerations, contractual obligations, or notice on a specific document.



SECURITY CLASSIFICATION OF THIS PAGE (When Data Entered)

19 REPORT DOCUMENTATION PAGE		READ INSTRUCTIONS BEFORE COMPLETING FORM
1. REPORT NUMBER 18 AFAPL TR-77-82	2. GOVT ACCESSION NO.	3. RECIPIENT'S CATALOG NUMBER 9
4. TITLE (and Subtitle) 6 ELECTRON TRANSMISSION THROUGH A VIBRATIONALLY EXCITED GAS	5. TYPE OF REPORT & PERIOD COVERED Final Report 9 Dec 74 - 16 May 77	
7. AUTHOR(s) 10 Charles A. DeJoseph, Jr/	8. CONTRACT OR GRANT NUMBER(s) 15 F33615-75-C-1082	
9. PERFORMING ORGANIZATION NAME AND ADDRESS Universal Energy Systems, Inc. 3195 Plainfield Road Dayton, Ohio 45432	10. PROGRAM ELEMENT, PROJECT, TASK AREA & WORK UNIT NUMBERS 16 2301-52-78 17 50	
11. CONTROLLING OFFICE NAME AND ADDRESS Air Force Aero Propulsion Laboratory (POD) Air Force Systems Command Wright-Patterson AFB, Ohio 45433	12. REPORT DATE 11 December 1977	
14. MONITORING AGENCY NAME & ADDRESS (if different from Controlling Office) 12/65p.	13. NUMBER OF PAGES 65	
15. SECURITY CLASS. (of this report) Unclassified		15a. DECLASSIFICATION/DOWNGRADING SCHEDULE
16. DISTRIBUTION STATEMENT (of this Report) 61102 F Approved for public release; distribution unlimited		
17. DISTRIBUTION STATEMENT (of the abstract entered in Block 20, if different from Report)		
18. SUPPLEMENTARY NOTES		
19. KEY WORDS (Continue on reverse side if necessary and identify by block number) Electron Scattering, Total Scattering, Vibrationally Excited, Electron Transmission, Temporary Negative Ion		
20. ABSTRACT (Continue on reverse side if necessary and identify by block number) Abstract - Task III - A low energy electron spectrometer known as LEEMA (low energy electron monochromatic analyzer) was modified for the study of pre-excited gases. The means for pre-excitation was a low power S-band microwave cavity. Following modifications to the system, the electron transmission through vibrationally excited nitrogen was determined over the energy range 1 to 3.5 eV. with .1 eV. resolution.		

DD FORM 1 JAN 73 1473 EDITION OF 1 NOV 65 IS OBSOLETE

SECURITY CLASSIFICATION OF THIS PAGE (When Data Entered)

390743

Gen

## FOREWORD

This report describes research performed by Universal Energy Systems, Inc., Dayton, Ohio. The work was conducted under Contract F33615-75-C-1082. "Investigations of Methods of Plasma Excitation", Task III "Electron Transmission Through a Vibrationally Excited Gas".

The work reported herein was performed during the period 9 December 1974 to 16 May 1977 at the in-house facilities of the High Power Branch (POD-2 Bldg. 450), Aerospace Power Division (PO), Air Force Aero Propulsion Laboratory, Air Force Wright Aeronautical Laboratories, Wright-Patterson Air Force Base, Ohio. The work was conducted by the author, Mr. Charles A. DeJoseph, Jr. Research Physicist. The report was released by the author in June, 1977.

ADDITIONAL FOR	
RTS	of the Section <input checked="" type="checkbox"/>
POD	of the Section <input type="checkbox"/>
APL	of the Section <input type="checkbox"/>
DISTRIBUTION, AVAILABILITY CODES	
SPECIAL	
A	

## TABLE OF CONTENTS

SECTION		PAGE
I	INTRODUCTION. . . . .	1
II	RESONANT SCATTERING . . . . .	5
III	DESCRIPTION OF EXPERIMENT . . . . .	12
IV	RESULTS . . . . .	35
	REFERENCES. . . . .	57

# LIST OF ILLUSTRATIONS

FIGURE		PAGE
1	Simplified Electron Transmission Experiment. . . . .	3
2	Resonant Scattering Mechanism in N <sub>2</sub> . . . . .	10
3	LEEMA Electron Spectrometer. . . . .	13
4	Simplified Diagram of LEEMA Electron Gun . . . . .	15
5	Effect of RPD Grid on Electron Energy Distribution . . . . .	15
6	Signals From MRPD and REM Mode With N <sub>2</sub> . . . . .	20
7	Double Modulation Wave Forms With Resulting Equations. . . . .	22
8	Double Modulation Signal From N <sub>2</sub> . . . . .	24
9	LEEMA Microwave Discharge Tube . . . . .	29
10	LEEMA Modified for Excited Gas Studies . . . . .	31
11	Analytic Representation of N <sub>2</sub> Total Scattering Cross Section . . . .	40
12	Computer Simulation of N <sub>2</sub> Derivative: T <sub>v</sub> = 300°K. . . . .	42
13	Computer Simulation of N <sub>2</sub> Derivative: T <sub>v</sub> = 1000°K . . . . .	43
14	Computer Simulation of N <sub>2</sub> Derivative: T <sub>v</sub> = 1500°K . . . . .	44
15	Computer Simulation of N <sub>2</sub> Derivative: T <sub>v</sub> = 2000°K . . . . .	45
16	Measured Derivative For Vibrationally Hot N <sub>2</sub> . . . . .	47
17	Measured Derivative For Vibrationally Cold N <sub>2</sub> . . . . .	48
18	Pressure Dependence of Signal From Second Minimum of N <sub>2</sub> Derivative .	52
19	Derivative Signal From "Normal" and "Pre-Excited" 50-50 N <sub>2</sub> -He Mix. .	53
20	Derivative Signal From "Normal: and "Pre-Excited 10-90 N <sub>2</sub> -He Mix . .	55

## SUMMARY

An existing low energy electron spectrometer known as LEEMA (Low Energy Electron Monochromatic Analyzer) was modified for the study of pre-excited gases. The design allowed the gas under study to be pre-excited in a low power S-band microwave cavity before entering the scattering region for study. The LEEMA was also modified to allow the derivative of the transmitted electron current to be monitored. Following these modifications, the device was used to study the electron transmission through vibrationally excited nitrogen in the energy range 1.0-3.5eV. This study lead to the observation of electron scattering taking place from vibrationally excited nitrogen in the  $v=1$  and  $v=2$  states. Energy resolution in the measurements was 0.1eV.



## SECTION I

### INTRODUCTION

While a significant data bank is available in the field of low energy electron scattering from ground state atoms and molecules, there are only a few reports on scattering from metastable target species.<sup>1-4</sup> With interest in high energy loading of gases for discharge lasers, the latter has become important. The displacement of significant cross sections to lower energies will alter the electron energy distribution with subsequent changes in the power loading of the vibrational manifold. One type of scattering experiment which would yield some of this needed data is the type usually referred to as an electron transmission experiment.<sup>5</sup> Electron transmission studies of gasses using nearly monoenergetic electron beams have become increasingly important in recent years with the discovery of temporary negative ion states in atoms and molecules.<sup>6</sup> These resonant states have been found to be important mechanisms for both electronic and vibrational excitation and have been shown to be the primary mechanism for direct ground state vibrational excitation in many molecular species.<sup>7</sup> Studies of this type have been performed on more than a dozen atoms and diatomic molecules,<sup>5,7</sup> and a few polyatomic species.<sup>6,8,9</sup> Until very recently this data only involved high resolution studies of ground state species, with apparently no data available on transmission through excited state gasses. Therefore, as a first step toward gathering data to fill this gap, a program was undertaken to measure the electron transmission through vibrationally excited nitrogen in the energy range 1.0 to 3.5 electron volts with about 0.1 electron volt resolution.



A simplified electron transmission experiment is shown in Figure 1. The experiment is the electron analogue of an optical absorption measurement using a monochromatic source. The collimated beam of electrons of energy  $E$  passing through the cell is attenuated according to the expression<sup>5</sup>

$$I(E) = I_0(E) \exp[-n\sigma(E)\Delta X], \quad (1)$$

where  $I(E)$  is the electron current leaving the cell,  $I_0(E)$  is the electron current entering the cell,  $n$  is the number density of gas particles in the cell,  $\Delta X$  is the path length through the cell, and  $\sigma(E)$  is the total scattering cross section of the particles at energy  $E$ . Such factors as cell geometry, stray electric and magnetic fields, and the finite energy spread of the beam alter the form of equation (1);<sup>10</sup> however, it essentially remains the basis for all electron transmission measurements. The exponential term, which depends on path length, species present, number density, and electron energy, is usually referred to as the electron transmission function. If a number of different species is present in the cell, the transmission function becomes<sup>11</sup>

$$g(E) = \exp[-\Delta X \cdot \sum_i n_i \sigma_i(E)] \quad (2)$$

where the index  $i$  refers to the  $i^{\text{th}}$  species and  $n$  and  $\sigma(E)$  are as before. It can be seen from equations (1) and (2) that by measuring  $I(E)$  and  $I_0(E)$ , the transmission function  $g(E)$  can be determined. Then, in the case of a single scattering specie, if one knows the

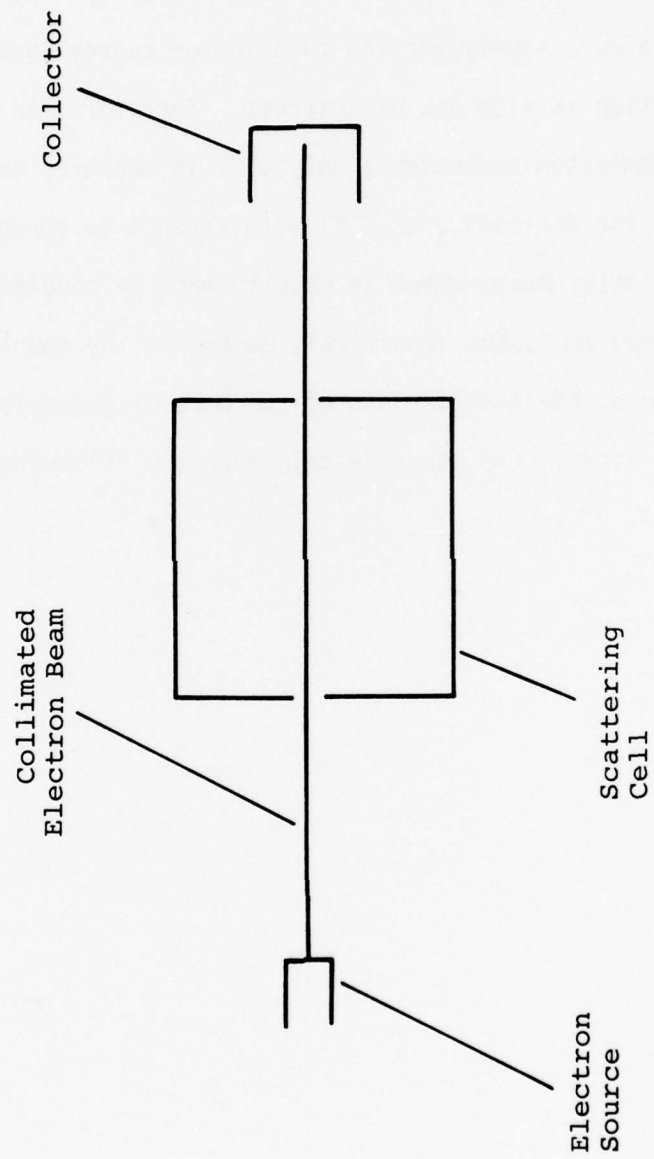


FIGURE 1 - SIMPLIFIED ELECTRON TRANSMISSION EXPERIMENT

number density  $n$  and the path length  $\Delta X$ , the total scattering cross section can be determined from  $g(E)$ .

In most high resolution transmission experiments only "fine structure" in the total scattering cross section is of interest, thus changes in  $g(E)$  that are slowly varying with energy are not important. Since  $I_0(E)$  is also a slowly varying function of energy (usually), this slow variation is also not of interest. Therefore, in most high resolution transmission experiments only  $I(E)$  is measured or, more desirably, only the derivative of  $I(E)$  with respect to energy is measured. The latter measurement is usually made by modulating the energy of the beam and phase sensitively detecting the modulated component. Both of these variations of the general transmission experiment were used in the study described on the following pages.

## SECTION II

### RESONANT SCATTERING

Resonances are responsible for producing sharp structure in a broad class of scattering experiments to which low energy electron scattering experiments belong.<sup>12</sup> This sharp variation in the cross section at some resonant energy  $E_R$  is related to the existence of a "nearly bound state"<sup>12</sup> of the projectile electron and the target atom or molecule. For this reason, the resonances that occur in low energy electron scattering are often referred to as temporary negative ion resonances. A number of excellent reviews on this type of scattering phenomenon have been presented from both a theoretical and experimental point of view. Burke<sup>13</sup> and Smith<sup>14</sup> have discussed the theory as applied to atoms while Bardsley and Mandl<sup>15</sup> have addressed molecular resonances. Taylor<sup>16</sup> has discussed the models, interpretations and calculations associated with the process for both atoms and molecules. Excellent reviews of the experimental data, along with some theory, have been given by Schulz for atoms<sup>5</sup> and diatomic molecules,<sup>7</sup> and very recently, for a number of species associated with laser plasmas.<sup>17</sup> A brief overview of the subject will be presented here, along with the specific details of the e-N<sub>2</sub> system. The discussion will rely heavily on the material presented in the aforementioned references. As mentioned earlier, the term "temporary negative ion resonance" is used to describe the resonances in electron-atom and electron-molecule scattering because the "nearly bound state" is one composed of the neutral target and the negatively charged projectile. At a particular energy,  $E_R$ , the projectile electron may become loosely bound in the "field" of

the target and become trapped for a time long compared with the normal transit time. The "field" may result from exchange forces, polarization forces, or some other forces resulting from the presence of the projectile. This results in a quasi-bond system of target and projectile, which decays via emission of the electron. Thus, the state is an autoionizing state. The time dependence of the wave function,  $\psi$ , of such a system can be written<sup>15</sup>

$$\psi \propto \exp(-iW_R t / \hbar)$$

with complex energy

$$W_R \equiv E_R - \frac{1}{2}i\Gamma_R.$$

Then

$$|\psi|^2 \propto \exp(-\Gamma_R t / \hbar)$$

where  $\hbar$  is Planck's constant divided by  $2\pi$ ,  $E_R$  is the energy of the resonance, and  $\Gamma_R$  is called the width of the resonance. Thus, the state decays with a lifetime of  $\hbar/\Gamma_R$ . Lifetimes for these temporary states normally range from approximately  $10^{-16}$  to  $10^{-12}$  seconds,<sup>5,7</sup> however, isolated cases might exceed these limits. Since bound states of atoms and molecules typically have lifetimes on the order of  $10^{-9}$  to  $10^{-7}$  seconds, it is clear that these temporary states do not fall into the range normally assigned to bound systems. The corresponding widths of these states range from about 1eV to  $10^{-4}$ eV.

Resonances in electron scattering can be classified into two categories which Taylor calls Type I and Type II.<sup>18</sup> The classification is based on the energy at which the resonance occurs relative



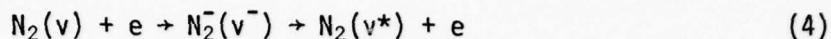
to an excitation threshold of the target. Type I, which are also known as Feshbach, compound state, or hole-particle resonances, occur at energies roughly 0.5eV below an excitation threshold of the target. The excitation threshold here normally belongs to an electronic state of the target; however, the threshold can belong to a vibrational level of the electronic ground state of a molecule. Bardsley<sup>15</sup> refers to these states as nuclear-excited Feshbach resonances. Mechanistically, the projectile electron can be imagined to excite an outer electron to a higher level, thereby creating a "hole" in the core electron cloud. This allows the projectile to "see" part of the nuclear field and become trapped in that field. The resonance then acts as a bound state relative to the excitation threshold of the outer electron.<sup>16</sup>

Type II resonances, which are also known as shape resonances, occur at energies above an excitation threshold of the target. The threshold can be an excited electronic state of the target or the ground electronic state. To date, however, no shape resonance associated with the ground electronic state of an atom has been observed.<sup>5,17</sup> Mechanistically, the projectile is trapped by a "centrifugal barrier" set up by a combination of its angular momentum component and the potential well it induces by exciting and polarizing the target."<sup>16</sup> With a few exceptions, Type II resonances are broader (i.e., shorter lived) than Type I because the trapping mechanism in the former is not as effective as in the latter. Since the barrier set up in the Type II resonance depends in part on the angular momentum of the projectile, no s-wave ( $\ell=0$ ) scattering is expected.<sup>12</sup> Thus, the angular



dependence of the scattered electrons also differs in many cases for the two types. These differences are important because, in many cases, the energy at which the resonance occurs is not enough alone to classify the type. Under conditions of closely spaced excitation thresholds it may be difficult to determine whether a resonance lies above one threshold or below another.

Resonances occurring in electron-molecule scattering generally yield more structure in a particular cross section than those in electron-atom scattering because of the larger number of bound states of the target. If the resonance is longer lived than the time needed for the molecule to vibrate, the temporary state will possess quasi-vibrational levels which will contribute structure to the cross section. This structure can show up in elastic and inelastic scattering as well as total scattering cross sections. Whether the structure appears in a particular cross section depends on the relative contributions of the resonant and non-resonant components of the process. Shape resonances (Type II) in electron-molecule scattering play an important role in vibrational and rotational excitation because these channels are "open" to the decay of the resonance. In nitrogen, for example, vibrational excitation is dominated by a shape resonance located near 2eV.<sup>7,15,16</sup> The non-resonant contribution to the process is small.<sup>7</sup> The negative ion formed is designated a  $2\Pi_g$  state,<sup>7</sup> and has a lifetime of the same order as one vibrational period of  $N_2$ .<sup>19</sup> Since the resonance has a lifetime roughly equal to a vibrational period of  $N_2$ , the negative ion possesses quasi-vibrational levels. Therefore, low energy resonant scattering in  $N_2$  can be described by the reaction



where  $v^-$  refers to one of the quasi-vibrational levels of  $\text{N}_2^-$  and  $v$  and  $v^*$  refer to vibrational levels of  $\text{N}_2$ . If  $v=v^*$  the process is resonant elastic scattering. If  $v < v^*$  the process is resonant inelastic scattering, and if  $v > v^*$  the process is resonant superelastic scattering. Figure 2 shows a potential energy diagram taken from Birtwistle and Herzenberg<sup>19</sup> which illustrates this scattering mechanism. The figure is a bit misleading since the vibrational levels of  $\text{N}_2^-$  are not true bound states. For example, from the diagram one would expect vibrational excitation cross sections for the lower few levels of  $\text{N}_2$  (which are resonant dominated) to exhibit peaks at energies given by the difference in energy between the  $\text{N}_2(v=0)$  ground state and the  $\text{N}_2^-(v^*)$  energy levels. What is observed, however, is that the peaks in the  $0 \rightarrow 1$  cross section are shifted in energy with respect to the  $0 \rightarrow 2$  cross section.<sup>7,19</sup> If the negative ion state were long lived compared to a vibrational period of  $\text{N}_2$ , each vibrational level of  $\text{N}_2^-$  would act like an isolated resonance and the diagram would accurately describe the resonant dominated cross sections. If the state were very short lived there would be no vibrational levels at all and Figure 2 would be completely erroneous. Since  $\text{N}_2^-$  falls into the intermediate case, the diagram should be taken as loosely describing the scattering mechanism. A further complication occurs in trying to predict the behavior of the elastic and total cross sections because of the large contribution from the non-resonant process.

The complex low energy electron scattering processes in nitrogen have been, to date, difficult to describe quantitatively. Much

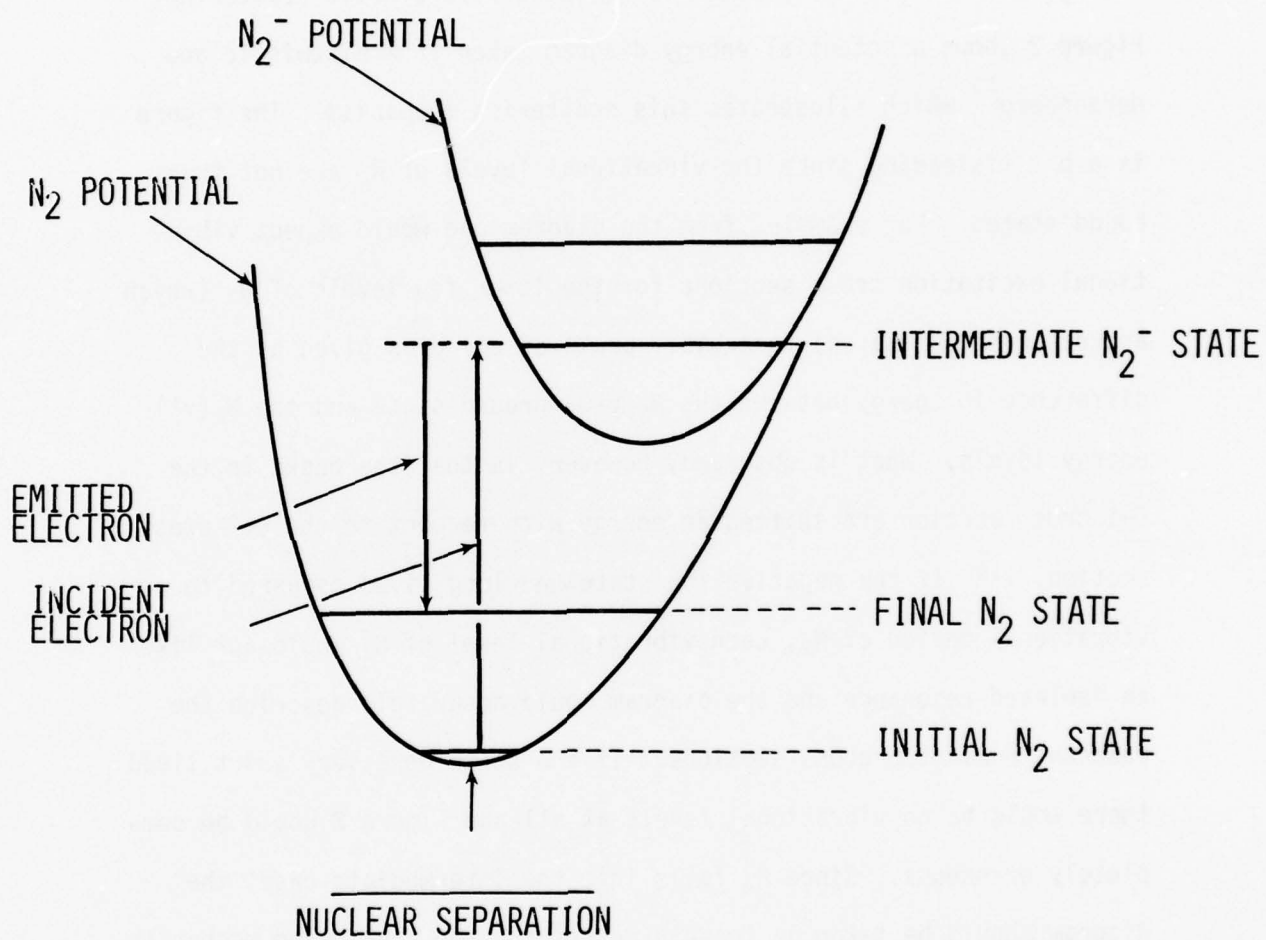


FIGURE 2 - RESONANT SCATTERING MECHANISM IN  $N_2$

experimental data exists,<sup>7</sup> but a theory that describes quantitatively the inelastic, elastic, and total cross sections has not appeared. Recently, Chandra and Temkin<sup>20</sup> have developed an approach that may prove capable of describing these cross sections and have compared their total scattering calculations with the measurements of Golden.<sup>21</sup> While their results are impressive, it appears there is still some work needed on the general theory. Birtwistle and Herzenberg<sup>19</sup> have developed a "boomerang" model that describes the inelastic scattering quite well; however, they have not attempted to account for non-resonant effects which are large in the elastic and total cross sections. Due to the lack of a theory that could accurately predict total scattering from ground state nitrogen, it was difficult to predict what the electron transmission through vibrationally excited nitrogen would be.

### SECTION III

#### DESCRIPTION OF THE EXPERIMENT

The experiment can be broken down into four subsystems: 1) an electron spectrometer capable of producing a near monoenergetic electron beam in the energy range of interest, 2) a scattering cell and associated gas-handling equipment to introduce the gas under study into the path of the electron beam, 3) the hardware and electronics necessary to detect and record the transmitted current, and 4) a means of vibrationally exciting the gas before it enters the scattering cell. The electron spectrometer and the detection subsystem are basically the same as described by Golden and Zecca,<sup>22</sup> but built by Advanced Research Instrument Systems, Inc. The A.R.I.S. spectrometer is known as the LEEMA, which stands for Low Energy Electron Monochromatic Analyzer. Figure 3 is a drawing of the LEEMA electron spectrometer. The scattering cell and collector are also shown to indicate their respective positions. The gun is cylindrically symmetric about the electron beam axis and is approximately 30.7cm in length and 2.2cm in diameter. All gun elements are OFHC copper and all apertures and grids are molybdenum. The various elements are mounted on two alumina rods using stainless steel clamps to form an "optical bench" configuration. The cathode and elements 1000 and 2000 serve to produce a well-collimated beam of electrons perpendicular to the 3000 element grid (retarding grid). The remaining elements are needed to produce a beam of small diameter and angular divergence over a wide range of final beam energies. In addition, elements 1000 and 6000 contain beam deflecting plates which can be used to correct beam alignment if necessary. The gun is housed inside a Molypermalloy



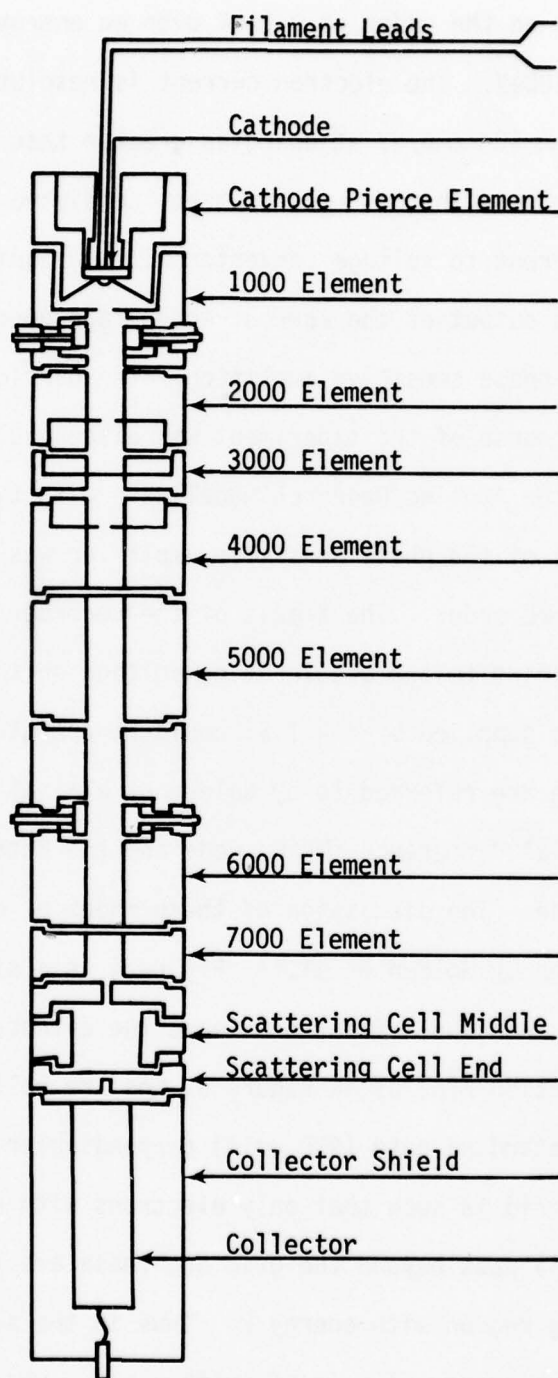


FIGURE 3 - LEEMA ELECTRON SPECTROMETER



magnetic shield since stray magnetic fields can degrade the performance of the device. The gun is capable of producing an electron beam with energy resolution on the order of 0.01eV over an energy range from 0 to greater than 100eV. The electron current is resolution dependent and goes roughly as  $10^{-7}$  amp/eV at energies greater than 1eV.<sup>22</sup> The collection subsystem used in these measurements consisted of a Faraday cup followed by a current to voltage converter with an equivalent resistance of  $10^7$  ohms. The output of the current to voltage converter was fed via ac coupling to a phase sensitive amplifier. The particular amplifier used during the course of the experiment was either an A.R.I.S. model 3000 or a Princeton Applied Research model HR-8 with type "C" preamplifier. The output of the phase sensitive amplifier was then fed to the Y-axis of an X-Y recorder. The X-axis of the recorder was driven by a voltage corresponding to the accelerating voltage on the electrons.

The LEEMA as supplied by A.R.I.S. could be operated in either of two modes. These are referred to by Golden et al.<sup>11</sup> as the Modulated Retarding Potential Difference (MRPD) mode and the Retarded Energy Modulation (REM) mode. The discussion of these modes of operation closely follows that given by Golden et al.<sup>11</sup> Figure 4 is a simplified diagram of the LEEMA electron gun. Electrons leave the cathode with some energy distribution function  $F(\epsilon)$  as in Figure 5, and are collimated so that most reach the retarding grid (RPD grid) perpendicular to it. The voltage on the RPD grid is such that only electrons with energy greater than  $E_1$  (Figure 5) pass beyond the grid and these are then accelerated to the scattering region with energy  $E$ . Thus in the scattering region the electrons have energy  $E' = \epsilon + E$ , with  $\epsilon > E_1$ , and the distribution function is given by  $F(E' - E)$ . When a gas is present in the scattering

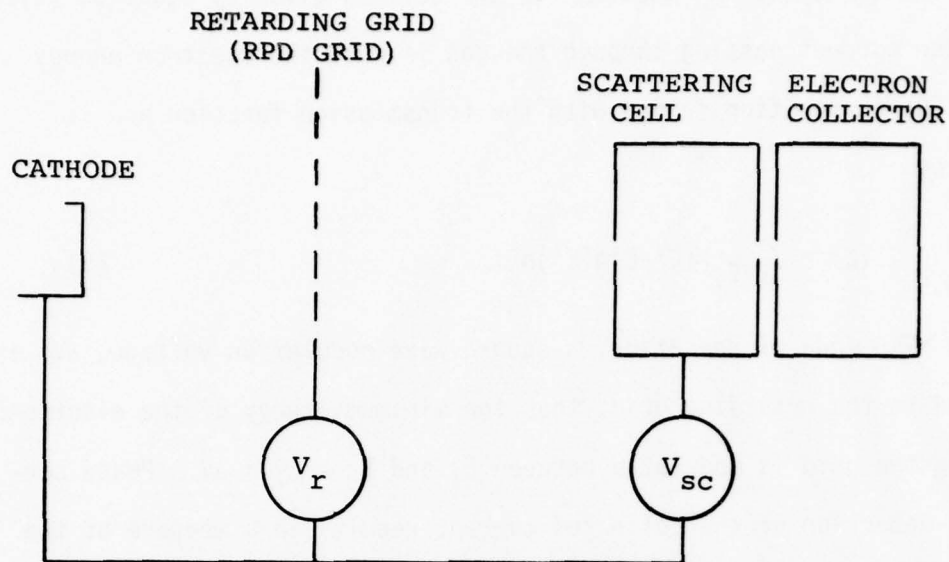


FIGURE 4 SIMPLIFIED DIAGRAM OF LEEMA ELECTRON GUN

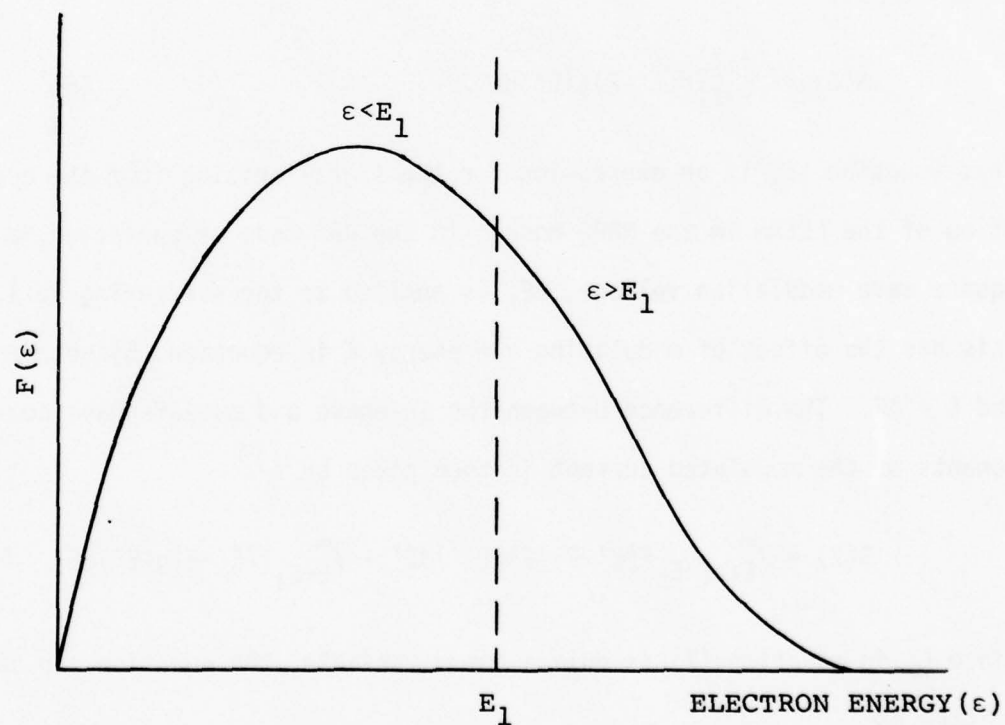


FIGURE 5 EFFECT OF RPD GRID ON ELECTRON ENERGY DISTRIBUTION

cell, the transmission function for the cell is given by equation (2). Thus the current passing through the gas is just the electron energy distribution function folded with the transmission function and is given by

$$I(E) = \int_{E+E_1}^{\infty} F(E'-E)g(E')dE'. \quad (5)$$

In the MRPD mode of operation, a square wave modulation voltage,  $\Delta V$ , is applied to the retarding grid; thus the minimum energy of the electrons passing the grid is modulated between  $E_1$  and  $E_2 = E_1 + \Delta V$ . Phase sensitive detection of the collected current results in a measure of the difference between the two signals, thus the measured signal is

$$S(E) = \int_{E+E_1}^{\infty} F(E'-E)g(E')dE' - \int_{E+E_2}^{\infty} F(E'-E)g(E')dE',$$

which is just

$$S(E) = \int_{E+E_1}^{E+E_2} F(E'-E)g(E')dE'. \quad (6)$$

Thus equation (6) is an expression for the signal arising from the operation of the LEEMA in the MRPD mode. In the REM mode of operation, a square wave modulation voltage,  $\Delta E$ , is applied to the scattering cell. This has the effect of modulating the energy  $E$  in equation (5) between  $E$  and  $E + \Delta E$ . The difference between the in-phase and out-of-phase components of the modulated current is then given by

$$S(E) = \int_{E+\Delta E+E_1}^{\infty} F(E'-E-\Delta E)g(E')dE' - \int_{E+E_1}^{\infty} F(E'-E)g(E')dE' \quad (7)$$

Since  $E'$  in equation (7) is only a dummy variable, the equation can be written as

$$S(E) = \int_{E+E_1}^{\infty} F(E'-E)g(E'+\Delta E)dE' - \int_{E+E_1}^{\infty} F(E'-E)g(E')dE'$$

which is just

$$S(E) = \int_{E+E_1}^{\infty} F(E'-E)[g(E'+\Delta E)-g(E')]dE'. \quad (8)$$

Thus equation (8) is an expression for the signal arising from the operation of the LEEMA in the REM mode.

To get a better understanding of the two modes of operation, consider equations (6) and (8) in more detail. If, in equation (6) one allows the modulation voltage to become infinitesimal, i.e.,  $\Delta V$  goes to  $\delta V$  and  $E_2$  approaches  $E_1$ , then  $S(E)$  is given by

$$\lim_{\Delta V \rightarrow \delta V} S(E) = \delta V \cdot F(E_1)g(E+E_1).$$

In this limit note that  $\delta V \cdot F(E_1)$  represents a current, say  $I_0$ , of "monochromatic" electrons, so the equation can be written

$$\lim_{\Delta V \rightarrow \delta V} S(E) = I_0 g(E+E_1). \quad (9)$$

Thus, in the limit of infinitesimal modulation amplitude, the MRPD LEEMA signal is directly proportional to the transmission function,  $g(E')$ , only shifted in energy by an amount  $E_1$ . From equation (2) it is clear that  $g(E')$  depends in a simple way on the total scattering cross section of each gas component, so the MRPD mode of operation yields, in the limit of infinitesimal modulation, a direct measure of the relative total scattering cross section for a given gas component. Realistically, finite modulation, imperfections in electron beam focusing, and signal-to-noise limitations alter equation (9) in two ways. First of all the focusing properties of the electron gun lead



to a current incident on the scattering region that is energy dependent and second, the transmission function must be averaged over a finite "slice" of the electron energy distribution function. Thus a more realistic form for equation (6) is

$$S(E) = I_0(E) \{g(E+E_1)\}_{E_2, E_1} \quad (10)$$

where the brackets represent an average over the portion of the electron energy distribution function from  $E_1$  to  $E_2$ . By dividing by the no-gas transmitted current and keeping modulation voltages small, the MRPD signal given in equation (10) is still a direct measure to the transmission function and thus a measure of the total scattering cross section. Equation (8) in the limit of infinitesimal modulation voltage can be written by expanding the part of the integrand containing the transmission function in a Taylor series which leads to

$$\text{Limit}_{\Delta E \rightarrow \delta E} S(E) = \int_{E+E_1}^{\infty} F(E'-E) \left[ \frac{dg}{dE'} \delta E \right] dE'$$

or,

$$\text{Limit}_{\Delta E \rightarrow \delta E} S(E) = \delta E \int_{E+E_1}^{\infty} F(E'-E) \left[ \frac{dg}{dE'} \right] dE'. \quad (11)$$

Thus in the limit of infinitesimal modulation amplitude, the REM LEEMA signal is a function of the derivative of the transmission function. Note, however, that the derivative is averaged over a large portion of the electron energy distribution function; consequently the functional dependence of  $S(E)$  on  $dg/dE'$  is not simple. If  $g(E')$  does not change appreciably over the width of the electron energy distribution function, then the derivative will also not change appreciably, and from equation

(11)  $S(E)$  will be proportional to  $dg/dE'$ . If, however,  $g(E)$  changes rapidly over the width of the distribution function, these changes, while enhanced by the derivative term, will be somewhat "smeared" over the distribution function. The effect, therefore, of using the REM mode of operation is that gradual changes in  $g(E')$  contribute a small amount to the resulting signal while rapidly varying, or "sharp" structure tends to stand out. Figure 6 is an actual plot of the signals arising from the two modes of operation, covering the energy range 0-6eV in  $N_2$ . Note that the sharp structure in the transmission function is hardly visible in the MRPD curve with only a broad dip occurring, while in the REM curve the broad dip is not seen but the sharp structure is enhanced. The structure in the REM curve does not however simply relate to structure in the transmission function, thus the curve serves only to indicate the existence of such structure.

Each of the two modes of operation just discussed possesses desirable, but mutually exclusive, characteristics. The MRPD mode of operation yields a signal whose origin is clearly defined and yields meaningful information; however, it is somewhat insensitive to small changes in the transmission function which are important in the identification of resonance phenomena. The REM mode of operation, while being more sensitive to small changes in the transmission function, yields a signal (even in the limit of infinitesimal modulation) that defies meaningful interpretation in terms of quantities of interest. The Double Modulation (DM) mode of operation described by Schöwengerdt and Golden,<sup>23</sup> offers the most desirable characteristics of each. In this scheme, modulation voltages of frequency  $F_0/2$  are applied to both the RPD grid and the scattering cell  $90^\circ$  out-of-phase with respect to each other, while the phase



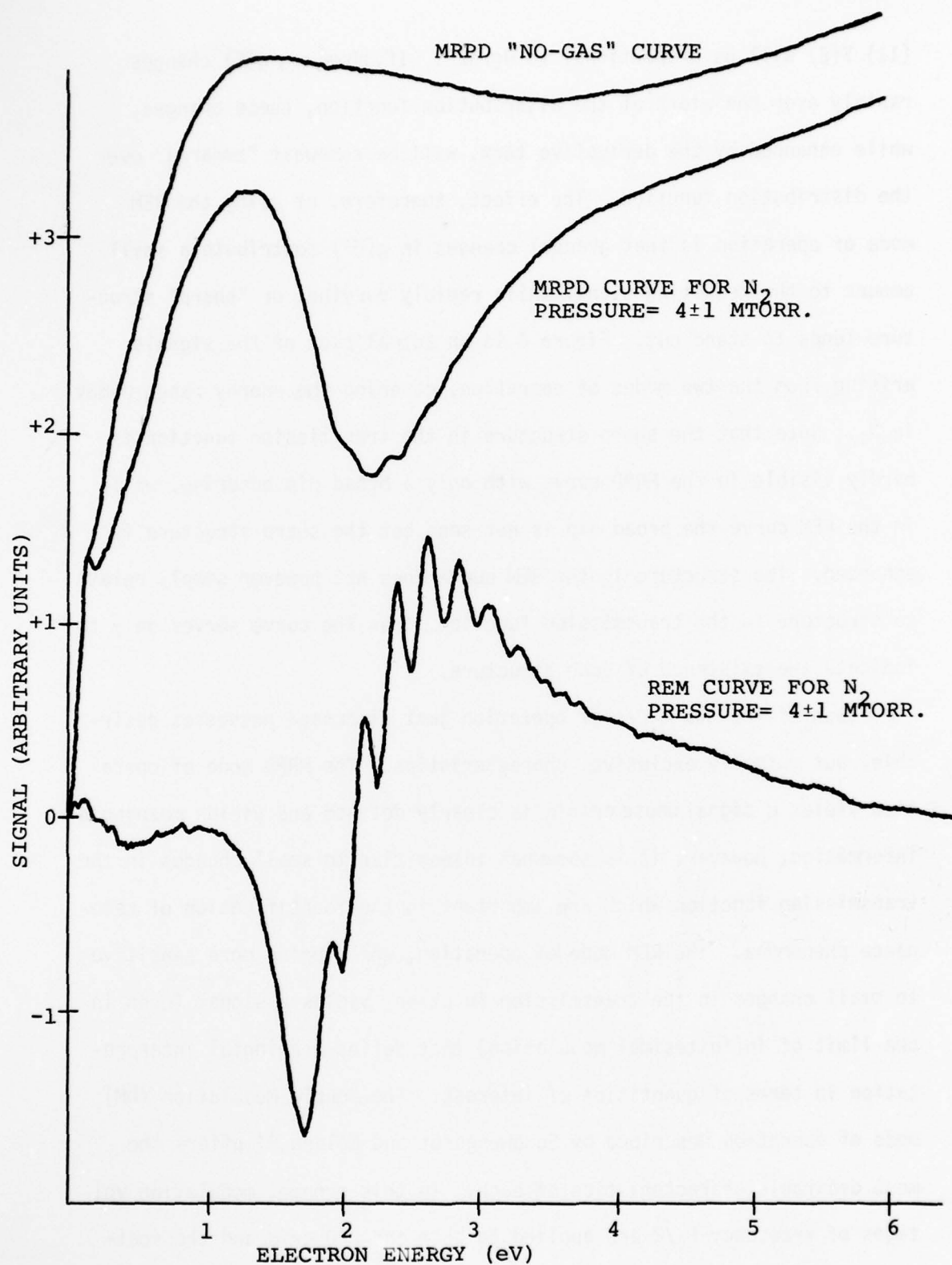


FIGURE 6. SIGNALS FROM MRPD AND REM MODE WITH N<sub>2</sub>

sensitive detector is referenced to frequency  $F_0$  (see Figure 7). The signals that result from each of the four regions follow from the earlier discussions and are labeled in Figure 7. With respect to the reference signal, the in-phase signals as registered by the phase sensitive detector are I + III, while the out-of-phase signals are II + IV. Thus the resulting difference signal is (I + III) - (II + IV) or (I - II) + (III - IV) which can be written

$$I - II = \int_{E+E_1}^{E+E_2} F(E'-E)g(E'+\Delta E)dE'$$

$$III - IV = \int_{E+E_2}^{E+E_1} F(E'-E)g(E')dE'$$

which gives

$$S(E) = \int_{E+E_1}^{E+E_2} F(E'-E)[g(E'+\Delta E) - g(E')]dE' \quad (12)$$

As before, let the modulation amplitudes  $\Delta V$  and  $\Delta E$  approach the infinitesimal amplitudes  $\delta V$  and  $\delta E$  and consider the form of equation (12). Expanding  $g(E' + \Delta E)$  in a Taylor series of first order in  $\Delta E$  yields

$$\text{Limit}_{\Delta E \rightarrow \delta E} S(E) = \delta E \int_{E+E_1}^{E+E_2} F(E'-E) \left[ \frac{dg}{dE'} \right] dE'$$

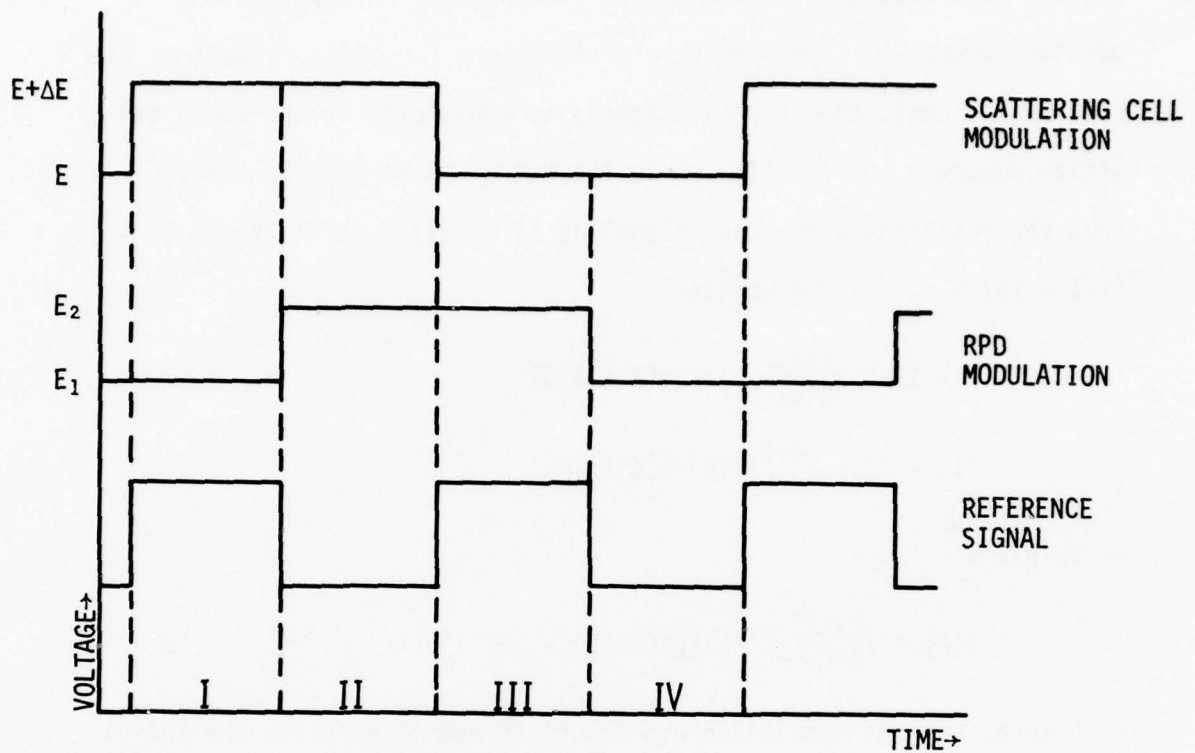
and as  $\Delta V$  approaches  $\delta V$ ,

$$\text{Limit}_{\substack{\Delta E \rightarrow \delta E \\ \Delta V \rightarrow \delta V}} S(E) = \delta E \cdot \delta V \cdot F(E_1) \frac{dg}{dE'} \bigg|_{E+E_1} \quad (13)$$

Letting  $\delta V \cdot F(E_1) = I_0$ , equation (13) can be written as

$$\text{Limit}_{\substack{\Delta E \rightarrow \delta E \\ \Delta V \rightarrow \delta V}} S(E) = \delta E \cdot I_0 \frac{dg}{dE'} \bigg|_{E+E_1} \quad (14)$$

Thus in the limit of infinitesimal modulation amplitudes, the DM mode



Region I:  $\int_{E+E_1}^{\infty} F(E'-E)g(E'+\Delta E)dE'$

Region II:  $\int_{E+E_2}^{\infty} F(E'-E)g(E'+\Delta E)dE'$

Region III:  $\int_{E+E_2}^{\infty} F(E'-E)g(E')dE'$

Region IV:  $\int_{E+E_1}^{\infty} F(E'-E)g(E')dE'$

DOUBLE MODULATION WAVEFORMS WITH RESULTING EQUATIONS

FIGURE 7

yields a signal that is directly proportional to the derivative of the transmission function. In reality, however, the signal suffers from the same problems as discussed earlier, thus a more realistic expression for the DM signal is

$$S(E) = \Delta E \cdot I_0(E) \left\{ \frac{\Delta g}{\Delta E} \right\}_{E_2, E_1} \quad (15)$$

Where, as before, the brackets indicate an average over the electron energy distribution function between  $E_1$  and  $E_2$ . Therefore the DM signal has the advantages of both a signal of relatively simple origin and high sensitivity to "sharp" structure in the transmission function.

The LEEMA electronics were modified to allow it to be operated in the DM mode, under the guidelines set up by Schöwengerdt and Golden.<sup>23</sup> Figure 8 shows a plot of the signal arising from a double modulation study of the structure in the  $N_2$  total scattering cross section in the range 0-6eV. It should be kept in mind that the signal is essentially a derivative of the transmission function, thus peaks in the curve do not correspond to peaks in the cross section. To see this more clearly, consider equation (2) for a single gas component. Substituting this expression into equation (14) gives, in the limit of infinitesimal modulation amplitudes

$$S(E) = -\delta E \cdot I_0 \cdot \Delta X \cdot n \cdot g(E+E_1) \frac{d\sigma}{dE} \Big|_{E+E_1} \quad (16)$$

Noting that  $g(E')$  is a slowly varying function of energy compared to the more rapidly varying derivative term, one can approximate the behavior of equation (16) by

$$S(E) \approx k \frac{d\sigma}{dE} \Big|_{E+E_1}$$

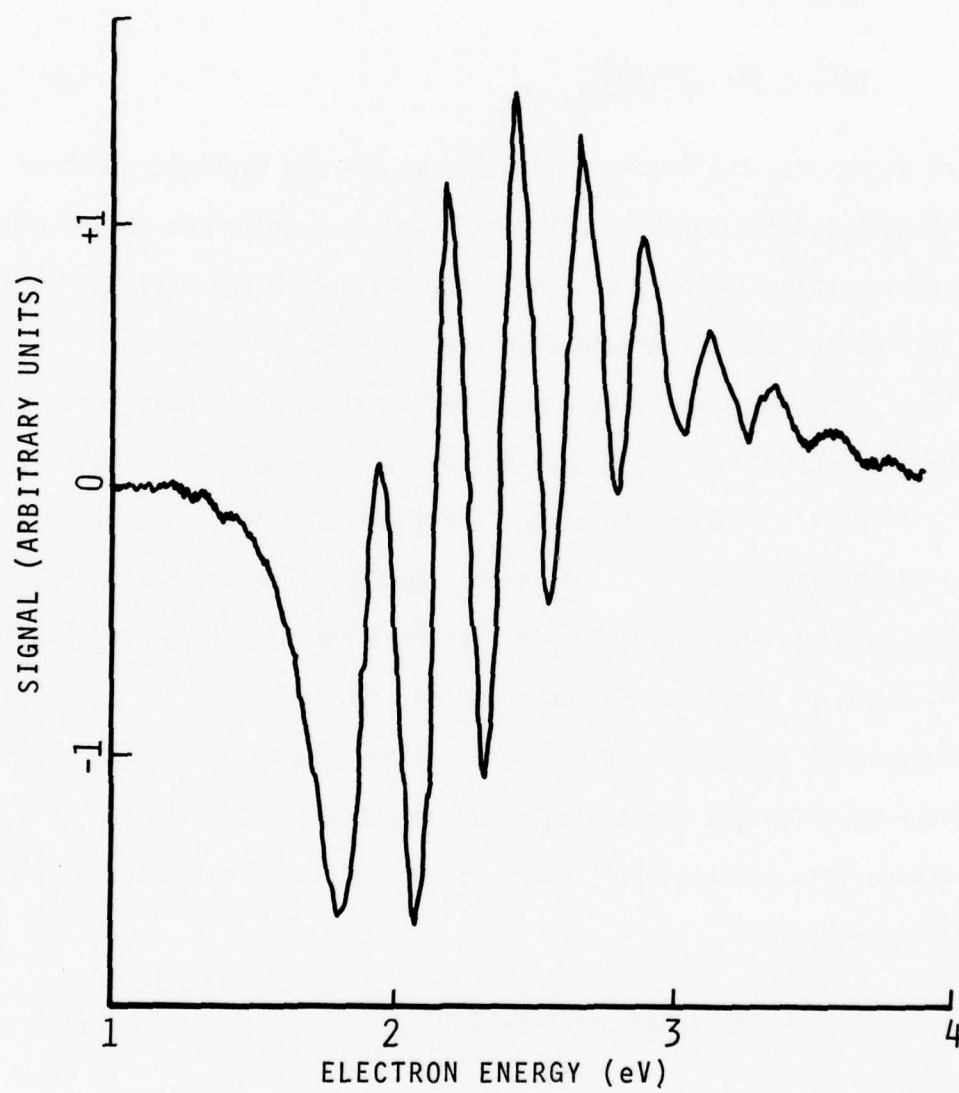


FIGURE 8 - DOUBLE MODULATION SIGNAL FROM  $N_2$



Thus,  $S(E)$  is roughly proportional to the negative of the derivative of the total scattering cross section. A minimum in  $S(E)$  indicates a point of maximum rate-of-increase with energy in the cross section, while a maximum in  $S(E)$  indicates a point of maximum rate-of-decrease in the cross section. Conversely, an extremum in the cross section is indicated by  $S(E) = 0$ .

The discussion of the DM mode of operation of the LEEMA has thus far been primarily concerned with the resulting signal under the conditions of infinitesimal modulation. As pointed out earlier, however, this is not a realistic situation; therefore, some mention of the effects of finite modulation amplitudes is in order. An exact expression for the functional dependence of  $S(E)$  on  $\sigma(E)$  is not possible in the case of finite modulation amplitudes since this requires one to know precisely the form of the electron energy distribution function at the scattering cell. However, some general procedures can be followed so that, to a recognized uncertainty, the curves follow the general behavior of equation (14). From equation (13) it can be seen that as either  $\delta E$  or  $\delta V$  approach zero, so does the signal. Therefore, the lower limits on the size of the modulation voltages are governed by the point at which the signal-to-noise ratio becomes intolerably small. This point is reached when the integration time for a measurement exceeds the confidence limits on the instrumental drift. At these lower limits one needs to consider two effects that result from the size of the modulation voltages. Since the "slice" of the electron energy distribution function in equation (15) is finite, the resolution of the instrument is also finite. Schöwengerdt and Golden<sup>23</sup> have studied this aspect of the DM mode and found that the resolution is approximately

equal to the average value of the two modulation amplitudes. The other consideration is how closely  $S(E)$  is to a true derivative of the transmission function. This, to a large degree, will depend on the form of  $g(E')$  which effects the accuracy of the Taylor expansion used in the derivation of equation (14). While these effects may appear independent, they are in fact intimately related. If, for example,  $g(E')$  varies slowly with respect to both modulation amplitudes, this implies that the Taylor series expansion is probably a good approximation, to first order in  $\Delta E$ , and the resolution will, by definition, be very good. Consequently, if the resolution of the instrument is very good, one can be reasonably certain that the signal closely follows the form of equation (14). In practice, one usually begins with large modulation voltages, then monitors the widths of any structure as the voltages are decreased. When the changes in width become insignificant with a decrease in modulation voltage,  $S(E)$  is assumed to very closely follow the form of equation (14). If this does not occur before the lower limits of modulation are reached, one must realize that the curve may deviate from a true derivative. In light of the aforementioned factors, consider the actual operating regime used to study  $N_2$ . The structure in the total scattering cross section at low energy for  $N_2$  is of the order of 200 millielectron volts (meV) in width and is clearly visible with modulation voltages at 200 milli-volts. However, resolution improves as the amplitudes are decreased until the voltages are about 50mV. At this point, improvement in resolution becomes insignificant. The lower limit for modulation while studying vibrationally cold  $N_2$  was about 20mV, however, with the gas pre-excited, an increase in noise raised this level to 50mV. Thus under these conditions one can be reasonably certain that the measured signal

closely follows the derivative of the transmission function. It was also found that best results were obtained by setting the two modulation voltages equal.

The original LEEMA spectrometer, scattering cell and collector were housed in a 304 (non-magnetic) stainless steel vacuum chamber equipped with ultrahigh vacuum feed-throughs for electrical connections to the gun elements. The chamber was evacuated using a Norton VHS-4 diffusion pump backed by a Welch 1402 mechanical pump. In addition, the diffusion pump was preceded by a liquid nitrogen and a zeolite trap to reduce backstreaming. The system was bakeable to 300°C and after bakeout achieved a base pressure on the order of  $10^{-9}$  torr. The gas supply system in the original configuration was designed to allow precise control of a very low mass flow of gas to the scattering region. Gas flowed out of the cell via the two small openings needed for the electron beam. For the study of pre-excited species it would be desirable to excite the gas and then instantly move the gas into the scattering region for study. This would insure the maximum number of excited species for study since there would be no time for deactivation. Since the gas cannot be moved instantly, an effort should be made to move the gas from the excitation region into the scattering cell in the shortest time possible. To do this high flow velocities are needed, coupled with the shortest distance possible from the excitation region to the scattering region. Thus, the modifications to the LEEMA were aimed at achieving these two goals without degrading the ultrahigh vacuum, ultraclean environment in which the electron gun, etc. were housed.

To help maintain a clean environment, an electrodeless discharge lamp was chosen for the excitation system. The specific device used

was an Evanson type microwave cavity<sup>24</sup> with modifications as suggested by McCarrol.<sup>25</sup> Microwave power was supplied by a Litton magnetron operating at 2.45GHz. With the power supplies available, the microwave supply was capable of 200 watts cw operation. Under these power conditions, the discharge tube which passes through the Evanson cavity had to be constructed of quartz because of its low microwave absorption. To use a quartz tube and maintain a bakeable configuration, quartz to metal seals were needed. Since direct quartz to metal seals are difficult to fabricate, glass to metal seals were further graded to quartz. To shorten the distance between the excitation region and the scattering cell, the inlet system was redesigned so that the path through the vacuum chamber to the scattering cell was as short as possible. A modified vacuum chamber was purchased with two side ports fitted with 2-3/4 inch flanges which allowed direct line-of-sight access to the scattering cell. In order to move the microwave cavity as close as possible to the scattering cell, a recessed "cup" was designed to allow the side arms of the McCarrol cavity<sup>25</sup> to extend into the chamber and thus come within about 15cm of the scattering region. Although the Evanson cavity<sup>24</sup> is more compact, it was felt that the McCarrol cavity offered better discharge stability, better power loading, and less chance of interference with detection electronics due to less radiated microwave power. After some fabrication problems developed with a Kovar "cup", the design was changed to make the "cup" an integral part of the discharge tube. Figure 9 shows the resulting design along with the connections to the scattering cell. The scattering cell used in the pre-excited gas study was modified from the original to allow pump out connections to be made and a



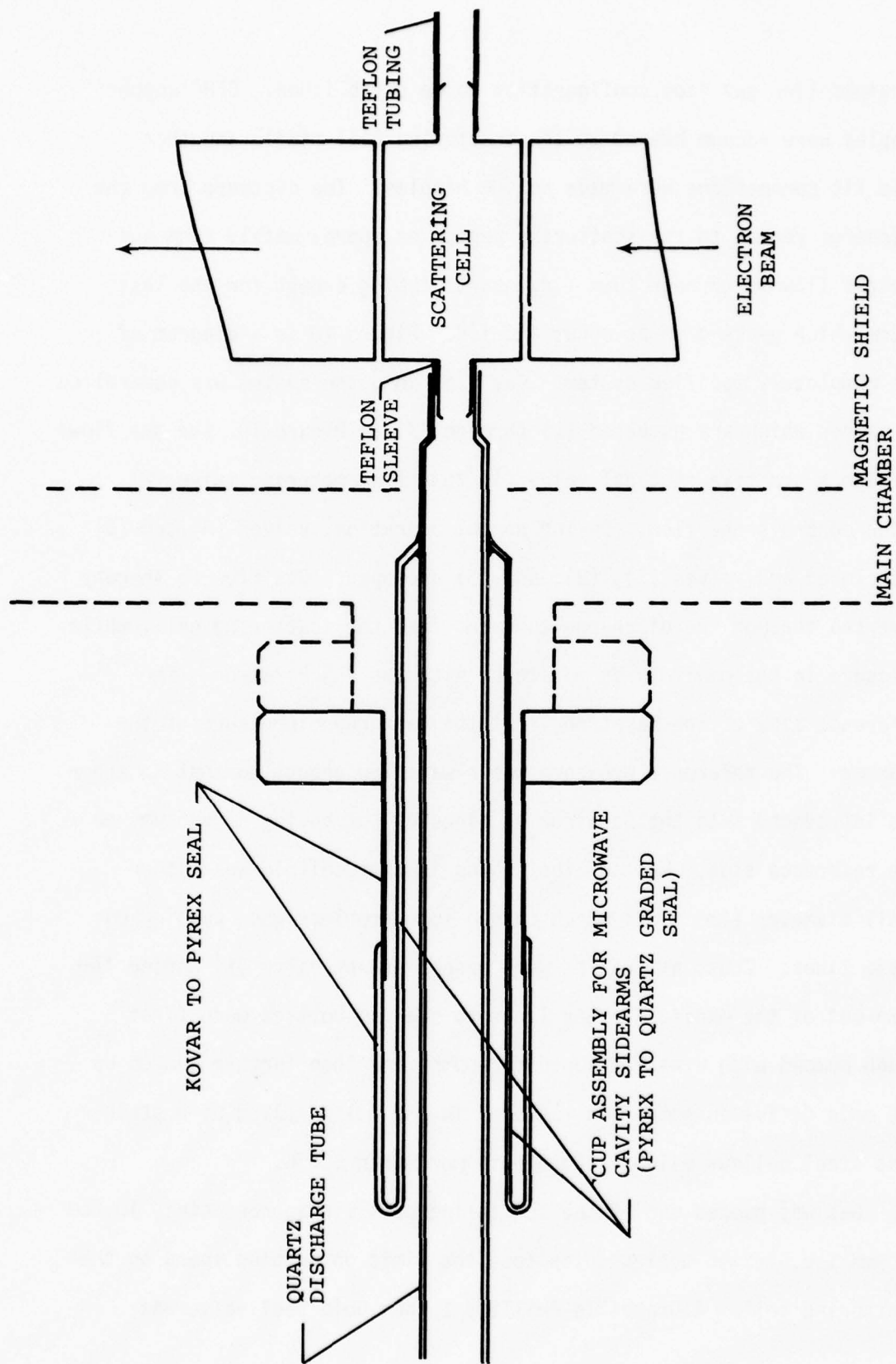


FIGURE 9 - LEEMA MICROWAVE DISCHARGE TUBE



straight-line gas flow configuration to be established. OFHC copper nipples were vacuum brazed to the scattering cell middle and then slip fit connections were made to the nipples. The distance from the discharge region to the scattering region is approximately 15cm and the gas flow is through 10mm i.d. quartz tubing except for the last 1.5cm which necks down to about 4mm i.d. Figure 10 is a diagram of the completely modified system. Gas flow into the system was controlled by valves which are numbered (1) through (7) in Figure 10. The gas flows through a positive shut off valve (1) to a fine metering valve (2) which controls the flow. During normal operation, valves (4) and (6) are closed and valves (5), (3), and (7) are open. Gas flow is thereby diverted through the discharge tube and into the scattering cell, while pressure in the manifold is monitored with the MKS Baratron. The reference side of the Baratron is at the background pressure of the chamber. The reference pressure was always low enough so that no error was introduced into the Baratron readings by not having a "vacuum" on the reference side. Most of the tubing in the manifold was rather small diameter (4mm i.d.) which caused some problems when pumping out these lines. Thus, all valves were opened except valve (1) during the pump-out of the manifold. Gas lines to the gas bottles were first rough pumped with a well-trapped forepump, and then further pumped by the main diffusion pump. Valves used in the inlet system were stainless steel bellows valves bakeable to more than 300°C.

Gas was pumped out of the scattering cell via approximately 10.2cm of 9mm i.d. Teflon tubing which sets the limit on pumping speed on the scattering cell. A Granville-Phillips 1 inch Gold Seal valve was

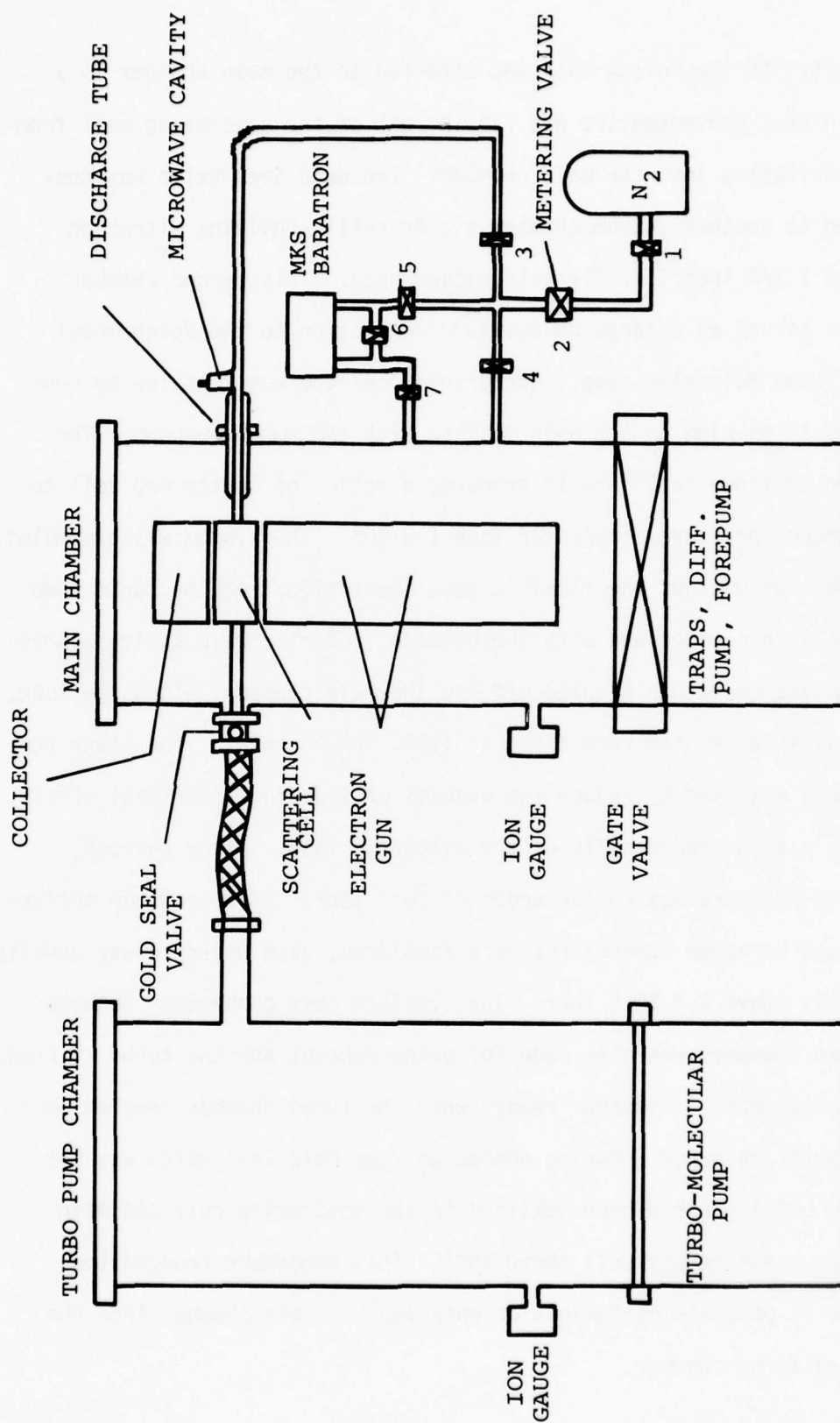


FIGURE 10 - LEEMA MODIFIED FOR EXCITED GAS STUDIES

connected to the Teflon tube and attached to the main chamber in a manner that prevented the gas flowing out of the scattering cell from back-diffusing into the main chamber. The Gold Seal valve was connected to another vacuum chamber via Granville-Phillips ultrahigh vacuum 1 1/2 inch i.d. flexible vacuum hose. This second chamber simply served as a large conductance connection to the Welch model 3102 Turbo Molecular pump. Background pressure was kept low by continuously pumping on the main chamber with the diffusion pump. The system as shown in Figure 10 produced a ratio of scattering cell to background pressure of greater than  $1 \times 10^4$ . The system was assembled for bakeout without the flexible hose connection from the turbo pump to the main chamber and with the Baratron and microwave cavity removed. All inlets were then blanked-off and the main chamber, discharge tube, and gas inlet system were baked at  $150^\circ\text{C}$  for 36 hours. The lower temperature was used to reduce the chances of inducing additional strain in the eleven graded seals of the discharge tube. After bakeout, chamber pressure was on the order of  $10^{-9}$  torr. After cathode activation and Baratron connections were completed, base pressure was usually slightly above  $1 \times 10^{-8}$  torr. The flexible hose connection between the two chambers was also made following bakeout and the turbo started. The system was considered "ready" when the turbo chamber reached  $10^{-8}$  torr pressure range. During operation, the Gold Seal valve was not opened until gas had been admitted to the scattering cell and main chamber pressure was well above  $10^{-8}$ . This procedure reduced the chance of possible contamination entering the main chamber from the unbaked turbo chamber.

The design of the gas handling system was aimed at achieving three goals. These were: 1) retain ultrahigh vacuum performance, 2) increase flow velocity between discharge region and scattering region, and 3) optimize operating conditions for a scattering cell pressure that maximized the derivative signal in  $N_2$ . The latter is found by differentiating equation (15) with respect to number density and setting the result equal to zero. This yields, for maximum signal,

$$n \Delta X \sigma = 1. \quad (17)$$

The total cross section in nitrogen near 2eV ranges from 1.0 to  $3.2 \times 10^{-15} \text{cm}^2$  according to Golden.<sup>21</sup> Taking  $\Delta X = 2.5 \text{cm}$ , the number density which maximizes the derivative signal is  $1.2 \times 10^{14} / \text{cm}^3 < n < 4.0 \times 10^{14}$  which at room temperature is equivalent to a pressure of  $4 \text{mtorr} < P < 12 \text{mtorr}$ . The first two goals were attained by following a number of general procedures, such as types of materials used, size of vacuum pump, etc. To achieve the latter goal required detailed flow calculations to be made over rather complex geometry. Additional problems arose in attempting to model gas flow in the system because, over the working pressure range, gas flow was neither molecular nor Poiseuille, but fell into the region Van Atta<sup>26</sup> calls the "transition region." At lower pressures, the flow should have been approximately molecular in nature, so molecular flow equations were used as a starting point. From these equations, the scattering cell pressure can be written

$$P(\text{scattering cell}) = K \cdot P(\text{Baratron}) \quad (18)$$

By measuring pressures in the main chamber, turbo chamber and at the

Baratron, and assuming reasonable values for the pumping speed in the turbo chamber, K could be determined. Calculations showed that equation (18) held reasonably well and that K was on the order of 0.1. Calculations also showed that the flow velocity out of the discharge tube was on the order of 200cm/sec. Since the precise pressure was not needed, the fact that equation (18) held reasonably well was all that was needed for the measurements.



## SECTION IV

### RESULTS

A first step in the measurement was to attempt to anticipate the signal that might arise from the presence of vibrationally excited nitrogen in the scattering cell. To precisely determine the signal expected, a knowledge of the total scattering cross sections for  $N_2(v>0)$  is required along with the population distribution in the scattering cell. Since only the general behavior of the derivative signal was desired, reasonable approximations for the above would suffice. Species entering the scattering region from a microwave discharge may include ions, metastables (electronically and vibrationally excited), and dissociation products.<sup>27</sup> In a nitrogen discharge, the only species which reached the scattering region in significant amounts are  $N_2(v\geq 0)$  and  $N$ .<sup>28</sup> The amount of  $N$  atoms reaching the scattering region is probably less than 1% of the  $N_2(v=0)$  number density,<sup>27</sup> so the predominate energetic nitrogen constituent should be  $N_2(v>0)$ . Due to  $v-v$  exchange collisions, the nitrogen vibrational level distribution in a microwave discharge is in general non-Boltzmann,<sup>29</sup> however the distribution of the lowest few levels can be adequately described by a Boltzmann distribution.<sup>30</sup> A number of workers have used low power microwave cavities of the type used in this work to vibrationally excite  $N_2$ , and have determined, at least, the  $v=1$  number density under a variety of experimental conditions.<sup>27,29,31</sup> The number density of  $N_2(v=1)$  molecules can be expressed as  $n(v=1)/n(v=0) = \exp[-\Theta/T_v]$ <sup>29</sup> where  $\Theta$  is the characteristic excitation energy of the first vibrational level of the molecule, and under the assumed Boltzmann

distribution over the lowest levels,  $T_v$  is the vibrational temperature. For  $N_2$ ,  $\theta = 3353.3^\circ K$  using the molecular constants from Herzberg.<sup>32</sup> The measurements of the number density of  $N_2(v=1, \text{ or higher})$  yield vibrational temperatures that vary from  $1000^\circ K$  to  $6000^\circ K$ , but more recent measurements<sup>29,31</sup> fall in the range of  $1000^\circ K$  to  $3000^\circ K$  and most of the data from reference 29 lies in the range of  $2000^\circ K$  to  $3000^\circ K$ . Thus it was assumed that the vibrational temperature of nitrogen in the discharge was between  $2000^\circ K$  and  $3000^\circ K$ .

To calculate the vibrational temperature of the gas in the scattering cell is a difficult problem. Since the nitrogen ground state does not possess a permanent dipole moment, the vibrational levels are metastable so the primary "cooling" mechanism in the experiment is wall deactivation. Unfortunately, the amount of wall deactivation is difficult to calculate because it is dependent on wall conditions, tube geometry, flow conditions, impurities in the gas, and a host of other variables.<sup>31</sup> Another problem is that the discharge is not a point discharge but tapers off for a considerable distance down the tube. In spite of these difficulties, a calculation was made following the outline of Black et al.<sup>31</sup> The discharge tube was assumed to behave as a 1.0cm diameter tube 13.5cm long followed by a .386cm diameter tube 1.5cm long. For a tube of  $r_0$ , Black et al<sup>31</sup> show that the equation governing the number density of the  $v=1$  level far downstream of the discharge is

$$n = R(r)\exp(-\alpha x/r_0) \quad (19)$$

where  $r$  is the radial coordinate,  $x$  is distance down the tube and  $\alpha$  is

the decay constant for the upper level. The differential equation for  $R(r)$  is

$$r_0^2(R'' + R'/r) + \alpha(\alpha + r_0 v/D)R = 0 \quad (20)$$

where  $v$  is the velocity of the gas and  $D$  is the constant interdiffusion coefficient. The boundary conditions on  $R$  are given by

$$R = 0 \text{ at } r = 0 \quad (21)$$

$$R + \delta r_0 R' = 0 \text{ at } r = r_0 \quad (22)$$

where

$$\delta = 4(1 - \gamma/2)D/\gamma \bar{c} r_0, \quad (23)$$

$\gamma$  is the deexcitation coefficient, and  $\bar{c}$  is the mean molecular speed. Black et al solve equation (20) for laminar Poiseuille flow; however, the conditions in this experiment are closer to molecular or slug flow. Thus in equation (20)  $v$  is replaced by  $v_0$  and the solution can be written<sup>33</sup>

$$R = C_1 J_0(\lambda r) + C_2 Y_0(\lambda r) \quad (24)$$

where  $J_0$  and  $Y_0$  are Bessel functions of the first and second kind and  $\lambda$  is given by

$$\lambda = [\alpha(\alpha + r_0 v_0/D)]^{1/2}/r_0 \quad (25)$$

Applying the boundary conditions (21) and (22) to equation (24) gives

$C_2 = 0$  and

$$J_0(\lambda r_0) - \delta r_0 \lambda J_1(\lambda r_0) = 0 \quad (26)$$

Equation (26) thus relates  $\alpha$ , the decay constant, to  $\gamma$ , the deexcitation coefficient, through equations (23) and (25). The solution of equation (26) was calculated as follows: Using the deexcitation coefficients measured by Black et al<sup>31</sup> for quartz and copper, and their interdiffusion coefficient,  $\delta$  was calculated. Then using this  $\delta$ , equation (26) was solved for  $\lambda$  by Newton's method.<sup>34</sup> The Bessel functions were evaluated by series at each point in the iteration. Using the tube sizes given and flow velocities of 200cm/sec in the large tube and 700cm/sec in the small tube, the result was that approximately 20% of the  $N_2(v = 1)$  molecules reach the scattering region from the discharge. It was felt, however, that due to the ultraclean system used in this experiment, the figure arrived at might well be the minimum survival figure. Using the minimum values for the deexcitation coefficients (staying within the estimated error) measured by Black et al, the percent that survive is found to be 50%. It is felt that this higher figure is probably closer to the true value, so taking an average of the two gives roughly a 35% survival figure. It should be stressed that the confidence in this figure is poor and the true value may differ from the above by a factor of 2 either way. Using the 35% survival figure, the resulting range of vibrational temperatures in the scattering cell is from 1300°K to 1547°K; however, due to the large uncertainty in the deactivation calculation, the range was extended from 1000°K to 2000°K. Thus the assumptions for the vibrational distribution in the scattering cell are 1) the distribution is Boltzmann and 2) the vibrational temperature ranges from 1000°K to 2000°K.

To predict qualitative behavior of the derivative signal with



vibrationally "hot"  $N_2$  in the scattering cell, approximations for the higher level cross sections are needed. Since no calculations existed at the time, it was assumed that the cross sections from the upper levels were the same size and shape as the ground state only shifted lower in energy. The reason for the shift to lower energy can be seen from Figure 2 and the discussion in section II. Since less energy is required to form the  $N_2^-$  state from a higher vibrational level of  $N_2$ , resonant phenomena should occur at lower energy. The amount each cross section was shifted was equal to the energy of the particular vibrational level above  $v = 0$ . To obtain an analytic representation of the  $v = 0$  cross sections, each vibrational level of  $N_2^-$  was treated as an isolated resonance and a modified Breit-Wigner<sup>35</sup> formula applied to it. Thus for the  $i^{th}$  level of  $N_2^-$ , the resonant cross section was written

$$\sigma_{i0}(E) = W_i \frac{\Gamma^2/4}{(E-E_{i0})^2 + \Gamma^2/4} \quad (27)$$

and the total scattering cross section for  $N_2(v=0)$  was written

$$\sigma_0(E) = \sum_i^N \sigma_{i0}(E). \quad (28)$$

In equation (27),  $\Gamma$  is the width of the resonance,  $E_{i0}$  is the energy of the resonance measured with respect to  $v = 0$  level of  $N_2$ , and  $W_i$  is an adjustable constant. The values for  $\Gamma$ ,  $E_{i0}$ 's, and  $W_i$ 's were obtained from a best fit to Golden's data<sup>21</sup> for  $N=7$  in equation (28). Figure 11 shows a plot of the function along with Golden's data taken from Kieffer.<sup>36</sup> While the function is seen to fit well in the central region, the fit is somewhat poorer in the "wings" of the cross section. For the higher level cross sections, equation (28) was generalized to



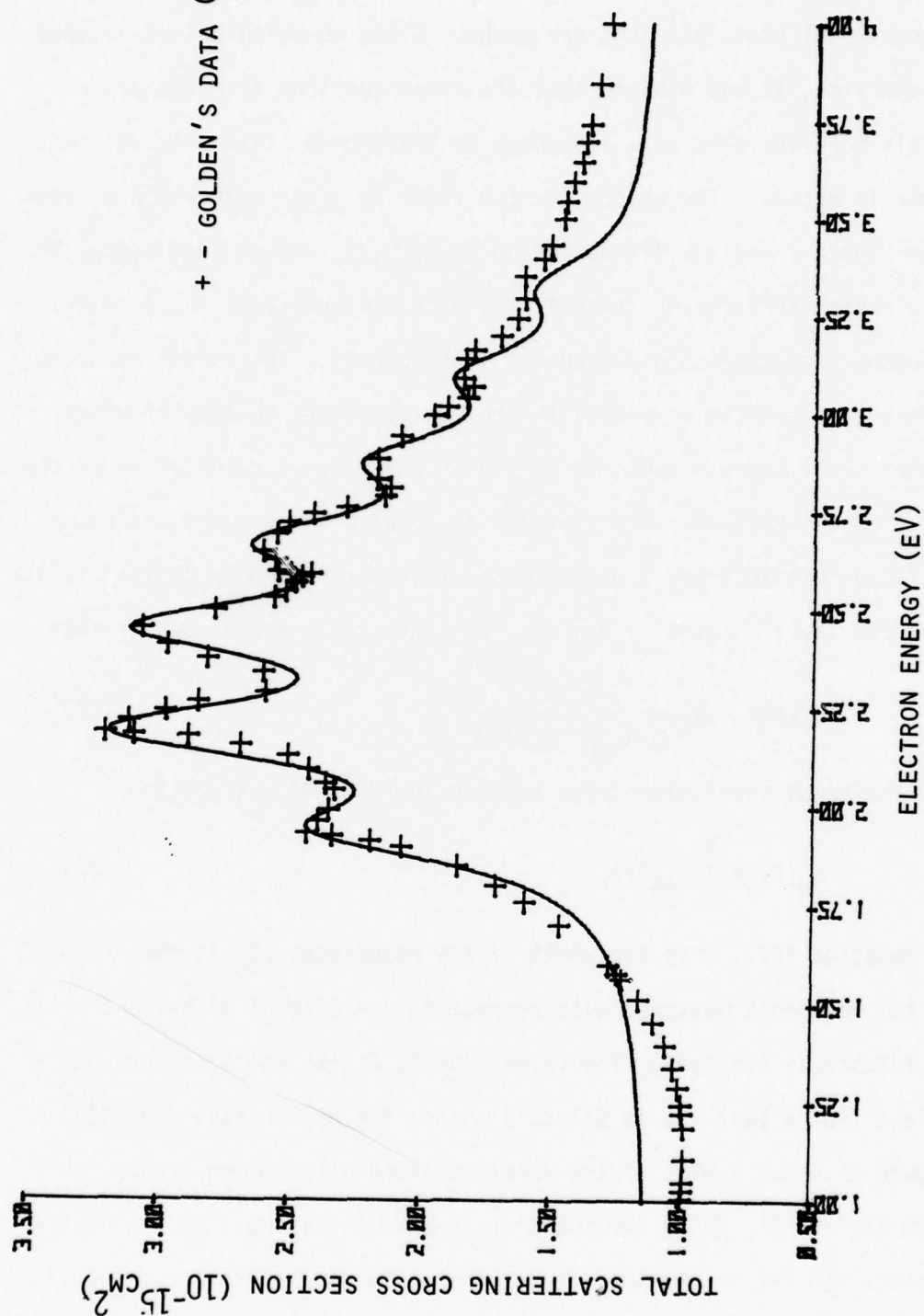


FIGURE 11 - ANALYTIC REPRESENTATION OF  $\text{N}_2$  TOTAL SCATTERING CROSS SECTION

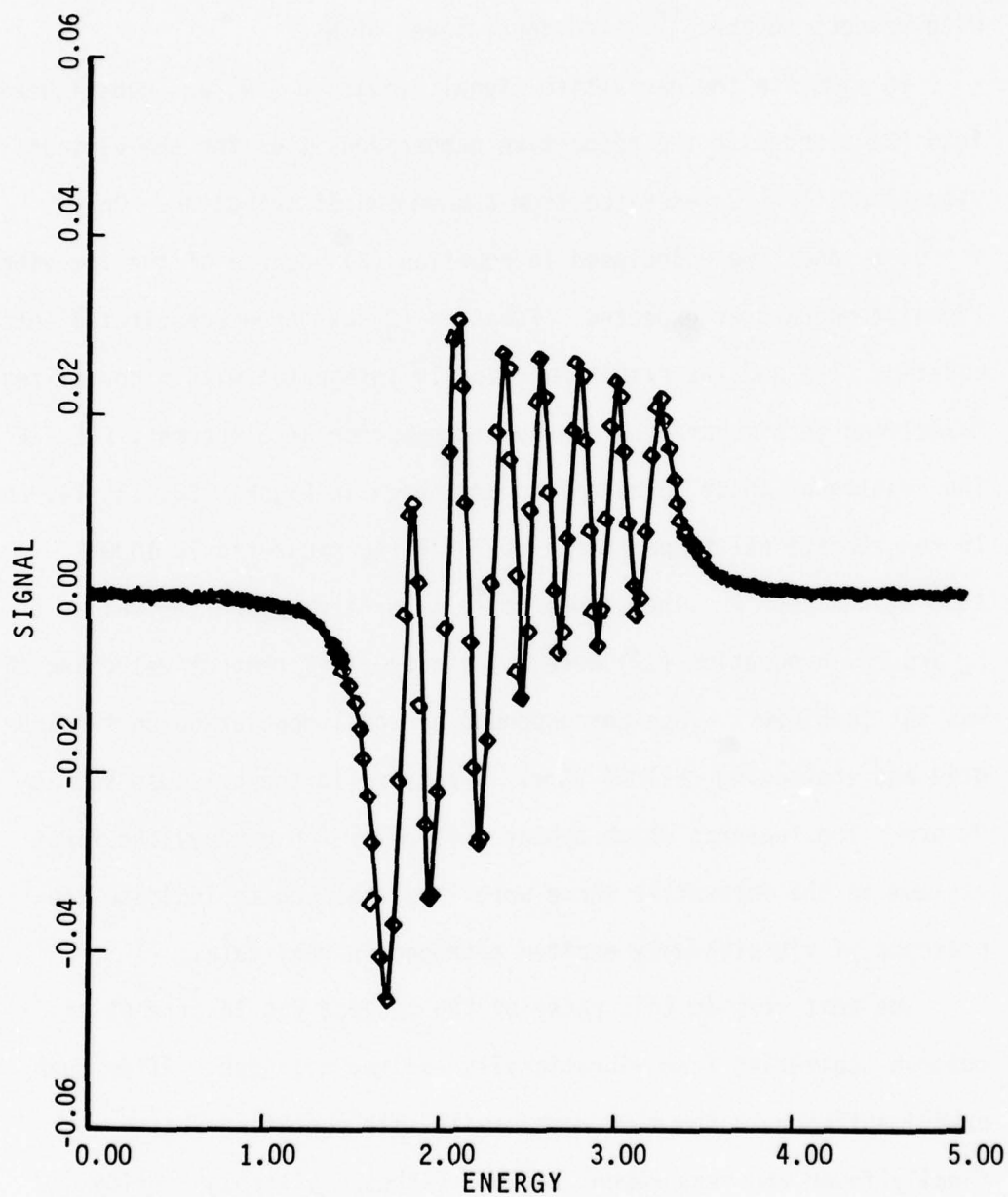
$$\sigma_j(E) = \sum_i^N \sigma_{ij}(E) \quad (29)$$

where the index  $j$  also generalized the energy term in equation (27) to  $E_{ij}$ . This term now represents the energy of the resonance measured with respect to the  $j^{\text{th}}$  vibrational level of  $N_2$ .

To simulate the derivative signal, equation (29) was substituted into (2) along with the respective number densities for the various vibrational levels generated from a Boltzmann distribution. Only  $v = 0, 1$ , and  $2$  were included in equation (2) because of the low vibrational temperatures expected. Equation (2) was then substituted into equation (12) and the result numerically integrated with a normalized Maxwellian to simulate the energy distribution of electrons,  $F(E - E')$ . The results of these calculations are shown in Figures 12, 13, 14, and 15 for vibrational temperatures of  $300^\circ\text{K}$  (no excitation),  $1000^\circ\text{K}$ ,  $1500^\circ\text{K}$ , and  $2000^\circ\text{K}$ . The signal scale is arbitrary and the values of  $E_1$  and  $E_2$  in equation (12) were  $0.1\text{eV}$  and  $0.15\text{eV}$ , respectively, and  $\Delta E$  was set to  $0.05\text{eV}$ . This corresponded to equal modulation on the RPD grid and scattering cell of  $50\text{meV}$ . Pressure in the cell was set at  $8\text{mtorr}$ . The features which appear just below (in energy) the first minimum in the derivative curve were thus expected to indicate the presence of vibrationally excited nitrogen in real data.

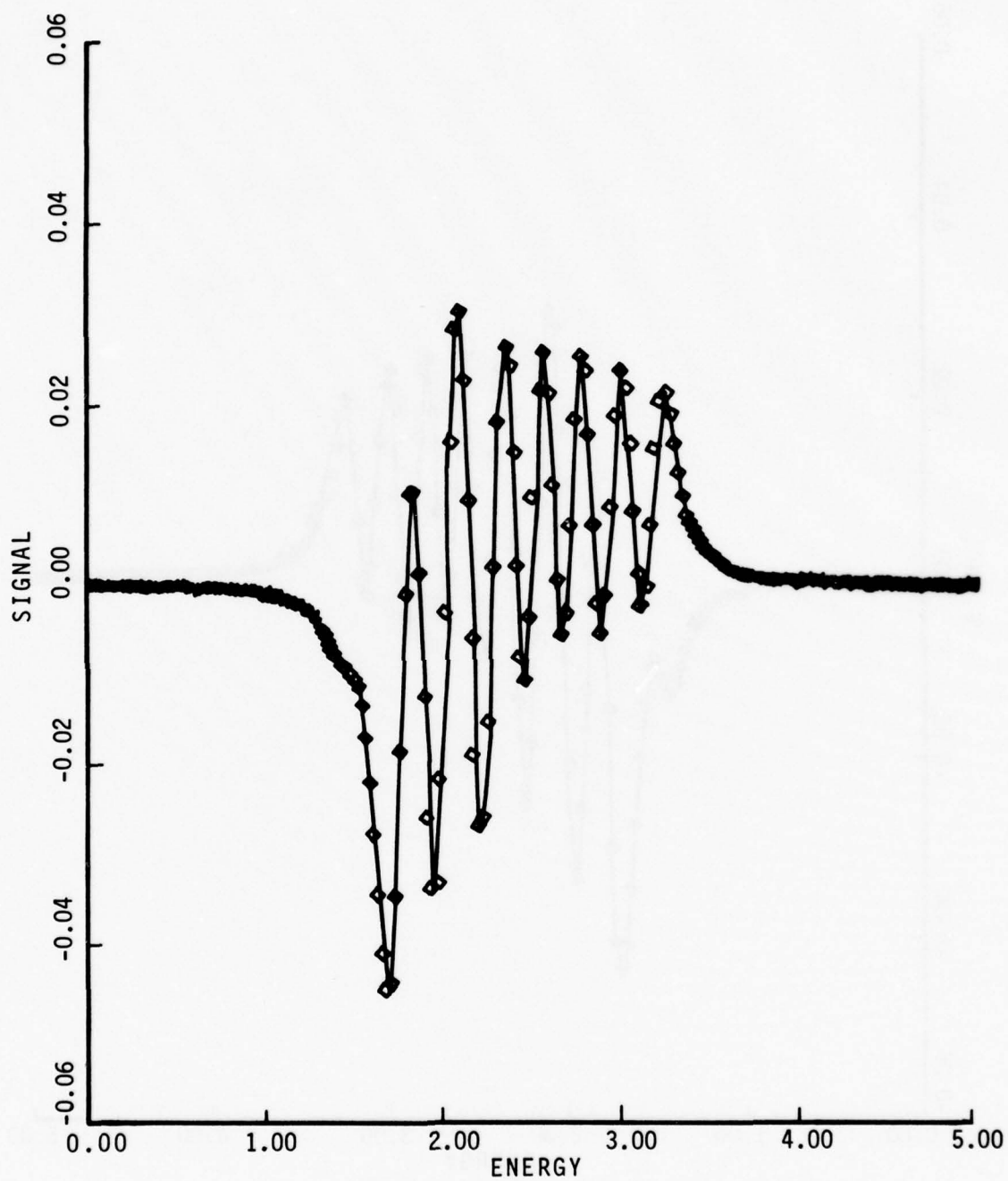
The next step in this phase of the project was to attempt to observe scattering from vibrationally excited nitrogen. After much experimenting with the microwave cavity, its operating regime was finally found and measurement begun. Matheson ultrahigh purity nitrogen was used, and with this gas it was found that a discharge could be maintained at a pressure above about  $10\text{mtorr}$  with about  $80$

78 12 26 116



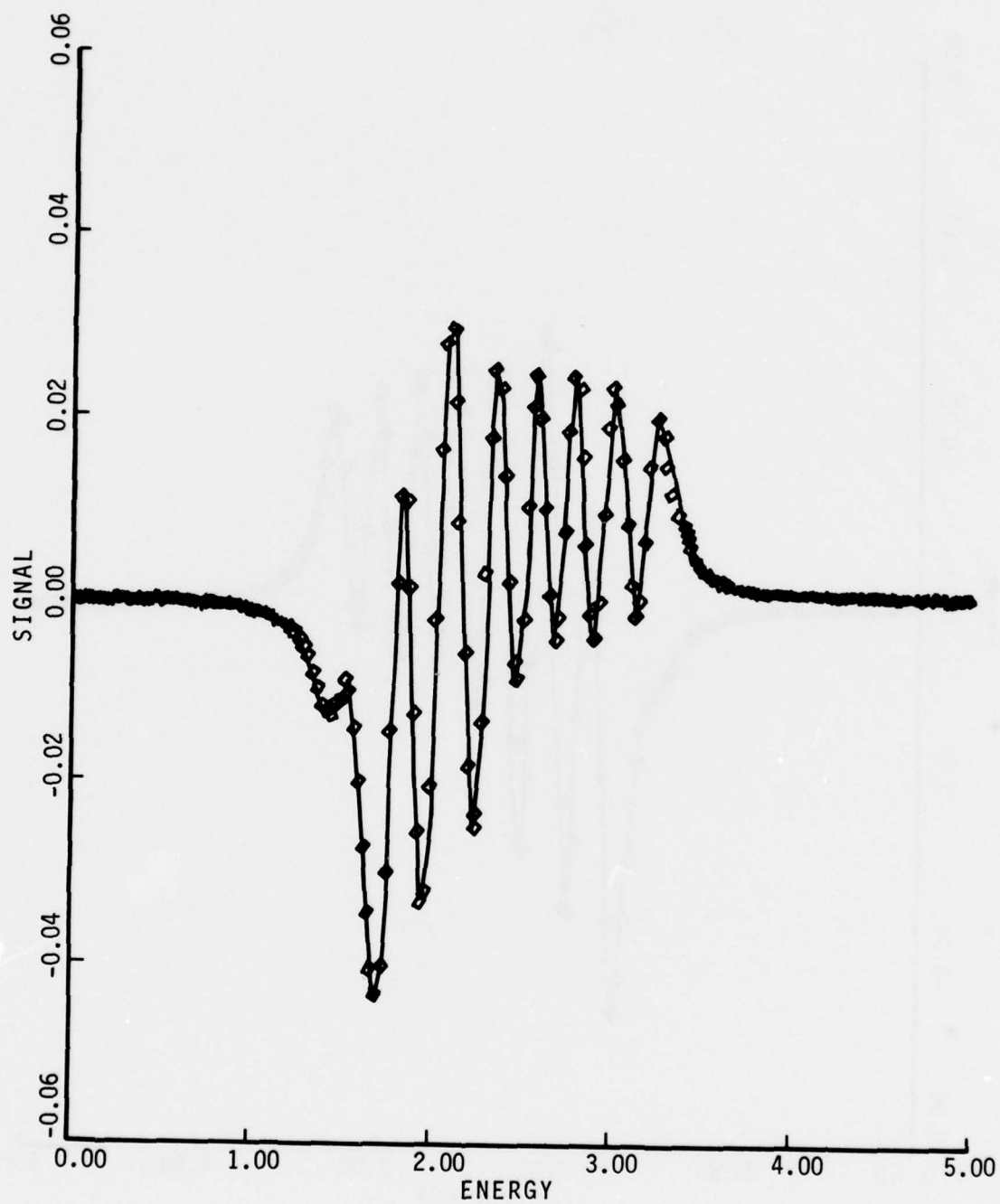
COMPUTER SIMULATION OF  $N_2$  DERIVATIVE:  $T_V = 300^\circ K$

FIGURE 12



COMPUTER SIMULATION OF N<sub>2</sub> DERIVATIVE: T<sub>v</sub> = 1000°K

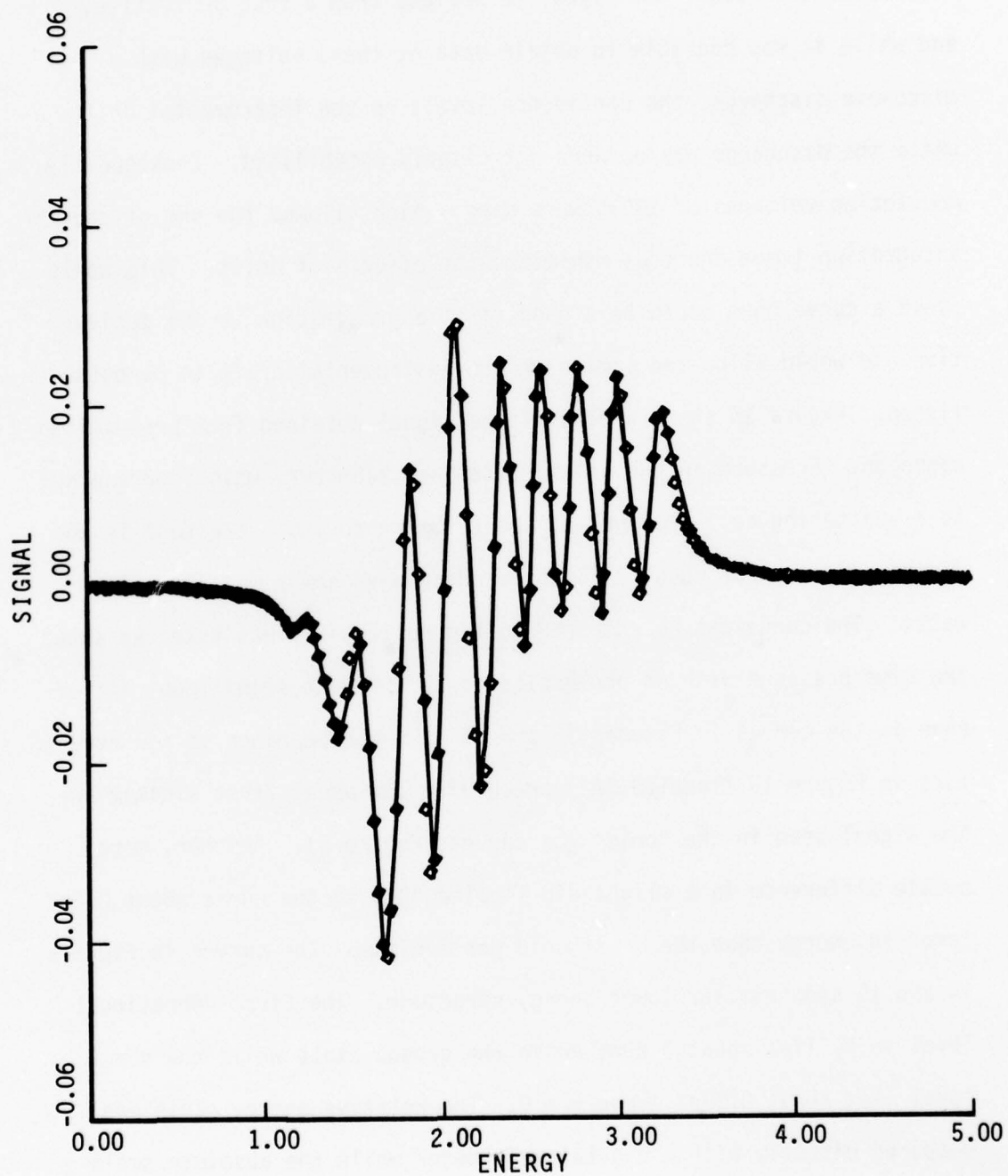
FIGURE 13



COMPUTER SIMULATION OF  $N_2$  DERIVATIVE:  $T_v = 1500^\circ K$

FIGURE 14





COMPUTER SIMULATION OF  $N_2$  DERIVATIVE:  $T_V = 2000^\circ K$   
FIGURE 15

watts of microwave power. As discussed earlier, modulation voltages above 50mV will cause the signal to deviate from a true derivative, and while it was possible to obtain data at these voltages with a microwave discharge, the confidence levels on the instrumental drift while the discharge was on were not clearly established. Consequently, modulation voltages of 100mV were used, which allowed the use of shorter integration times and thus minimized the effects of drift. This would yield a curve that would be a good first approximation to the derivative and would allow the limits on the instrumental drift to be established. Figure 16 shows a plot of the signal obtained from pre-excited nitrogen. Pressure in the inlet system was 145mtorr, which corresponds to a scattering cell pressure of about  $15 \pm 3$ mtorr and a pressure in the discharge region of about  $24 \pm 5$ mtorr. Microwave power was about 100 watts. The curve can be compared to Figure 17 which was taken at about the same pressure with no pre-excitation. The most significant difference in the curves in Figures 16 and 17 is the appearance of new structure in Figure 16 (labeled "A") preceeding the usual first minimum in the signal seen in the "cold" gas curves (Figure 8). Another, more subtle difference is a slight dip (labeled "B") in the curve about 0.5eV lower in energy than the first cold gas minimum. The curves in Figures 14 and 15 show similar lower energy structure. The first vibrational level in  $N_2$  lies about 0.29eV above the ground state while the  $v = 2$  level lies about 0.58eV above  $v = 0$ . The relative energy scale was measured directly with a digital volt meter while the absolute scale was fixed by considering the onset of current in the device as  $E = 0$ . This was also checked using the MRPD mode and comparing the energy at

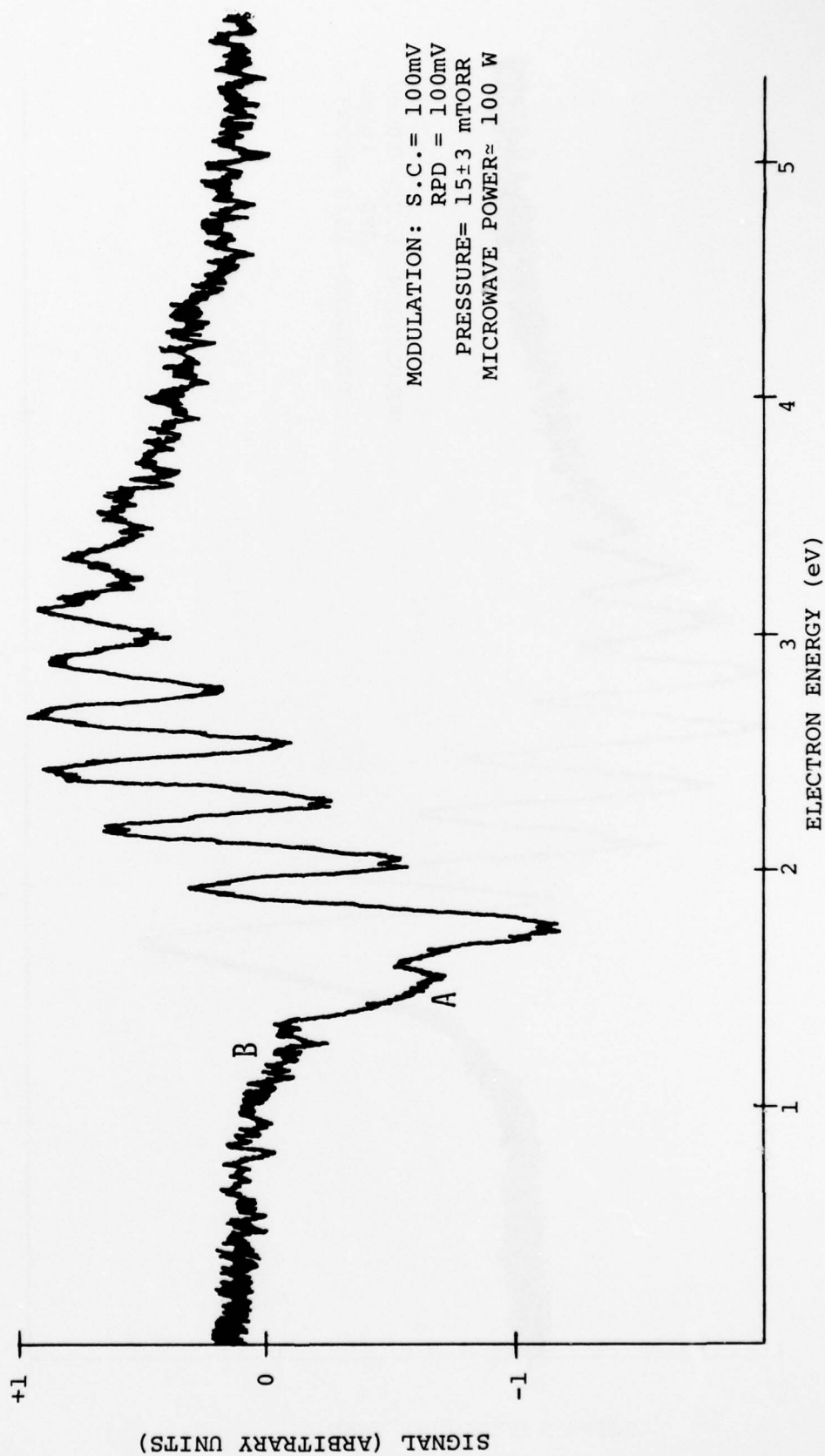


FIGURE 16 - MEASURED DERIVATIVE FOR VIBRATIONALLY "HOT" N<sub>2</sub>

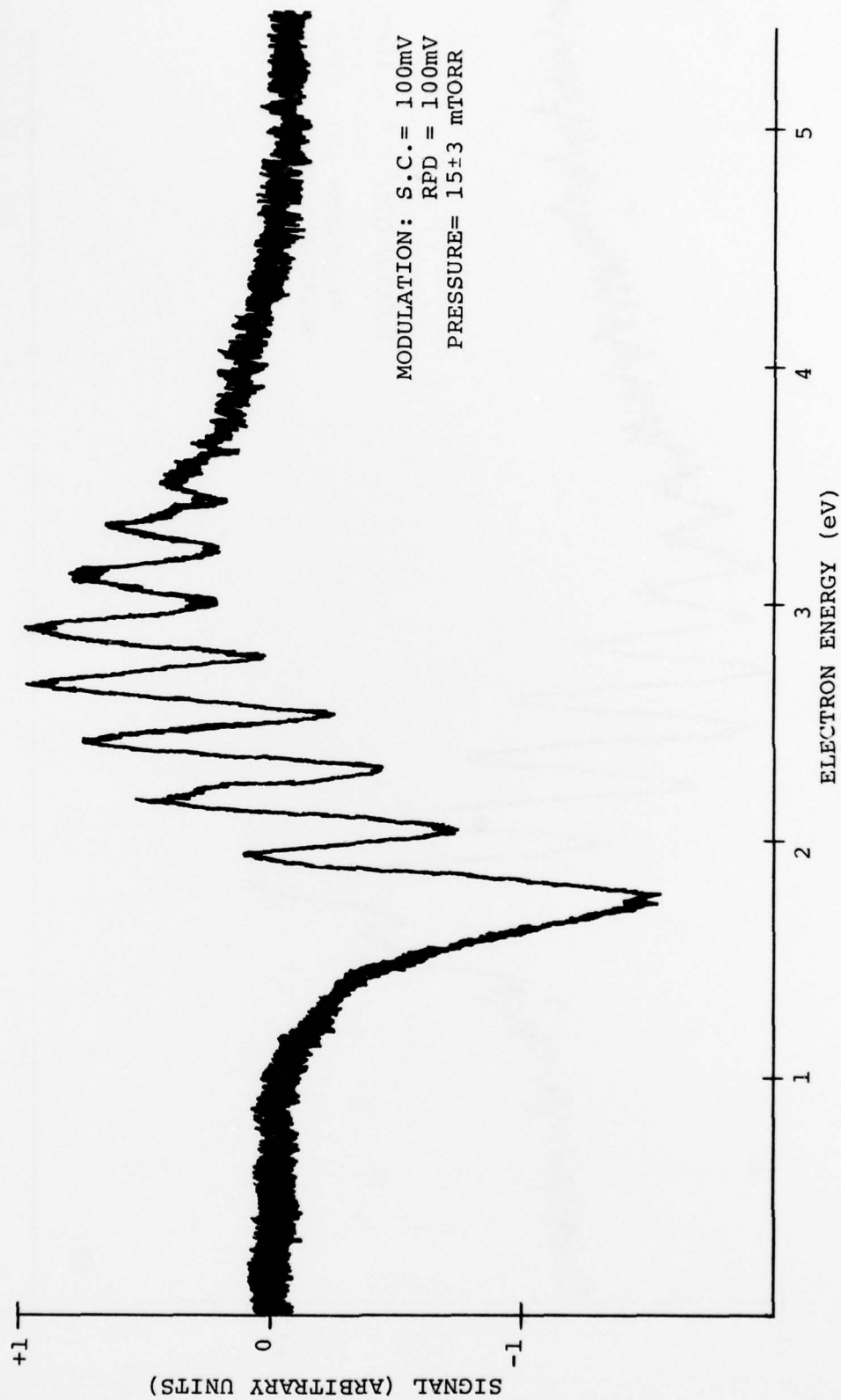


FIGURE 17 - MEASURED DERIVATIVE FOR VIBRATIONALLY "COLD"  $N_2$

which the second minimum in the transmission occurred with the second peak in Golden's cross section measurement.<sup>21</sup> The structure at "A" lies about 0.25eV below the first "cold" gas minimum, while the structure at "B" lies about 0.5eV lower in energy. Since the modulation voltages were set at 0.1eV, these values are within the instrumental uncertainty of the values of the vibrational spacing of N<sub>2</sub>. Thus it appeared that these structures were the result of scattering from vibrationally excited N<sub>2</sub>. The next step was to increase resolution and try to clearly resolve the structure. It was discovered at this point that two things had occurred: 1) The contact potential of the instrument had changed by about 0.3eV and 2) the no-gas transmission curve (equation (6) with  $g(E') = 1$ ) had changed drastically. It was found that the changes were permanent, and no amount of readjustment of the electron beam focusing could reverse them. Since this effect had not been observed previously, and the N<sub>2</sub> pressure during the run was the highest used with the microwave discharge on, it was felt that something from the high pressure discharge had contaminated the electron gun. Since the system had been baked and was considered clean ( $3 \times 10^{-9}$  torr), and the gas used was ultrahigh purity, it was suggested<sup>37</sup> that one possible cause for the changes was the reaction of atomic nitrogen, produced in the discharge, with the copper gun elements to form copper nitride. This would have the same effect as any surface contaminant whose conductivity differed from copper. Therefore it was decided to reduce the N<sub>2</sub> number density, yet still maintain a discharge, by using a 50-50 N<sub>2</sub>-He mix. The form of the double modulation signal from a gas mixture is found by substituting equation (2) into



equation (16) which yields

$$S(E) = -\delta E \cdot I_0 \cdot \Delta X \cdot g(E+E_1) \cdot \left\{ \sum_i n_i \frac{d\sigma_i}{dE} \right\} \Big|_{E+E_1}. \quad (30)$$

Golden and Bandel have measured the total scattering cross section for helium using modified Ramsauer technique, and find that in the range 0.2eV to 6.0 eV the cross section is almost constant and is approximately equal to  $5 \times 10^{-16} \text{cm}^2$ .<sup>38</sup> Therefore, the helium derivative term is approximately zero and equation (30) simplifies to

$$S(E) = -\delta E \cdot I_0 \cdot \Delta X \cdot g(E+E_1) \cdot n_{N_2} \frac{d\sigma_{N_2}}{dE} \Big|_{E+E_1}. \quad (31)$$

Thus, the shape of the curve from the  $N_2$ -He mix should be approximately the same as from pure  $N_2$ .

At this point it was decided to try to set better limits for the value of K in equation (18) and insure that the addition of helium had not drastically changed the flow characteristics of the system. The functional dependence of equation (31) on pressure can be written

$$S(E, n) \approx C_1(E) \cdot n \cdot \exp(-C_2(E) \cdot n) \quad (32)$$

where  $C_1$  and  $C_2$  are constants for a fixed energy.  $C_2(E)$  can be written

$$C_2(E) = \Delta X \cdot (\sigma_{N_2}(E) + \sigma_{He}(E)) \quad (33)$$

where  $\sigma_{N_2}$  and  $\sigma_{He}$  are the total scattering cross sections for  $N_2$  and He at energy E. In equation (32), n is the partial pressure of  $N_2$  in the scattering cell and can be written

$$n = K \cdot P_B(\text{mtorr}) \cdot 3.218 \times 10^{13} \quad (34)$$

where  $P_B$  is the partial pressure of  $N_2$  at the Baratron and  $K$  is the constant in equation (18). To determine  $K$ , the derivative signal was measured as a function of  $P_B$  at three different peaks in the signal. The data from each peak was then least-squares fit to the function

$$S = a \cdot P_B \cdot \exp(-b \cdot P_B) \quad (35)$$

and  $a$  and  $b$  determined. Figure 18 shows a plot of the data from the second minimum of the derivative signal (see Figure 8). From equations (32), (34), and (35) it can be seen that  $b$  is given by

$$b = C_2 \cdot K \cdot 3.218 \times 10^{13} \quad (36)$$

Values for  $C_2$  were determined from equation (33) using the  $\sigma_{N_2}$  values of Golden<sup>21</sup> and using  $\sigma_{He} = 5 \times 10^{-16} \text{cm}^2$  from Golden and Bandel.<sup>38</sup> The values determined for  $b$  and the corresponding values of  $C_2$  are shown below.

$$\text{1st minimum: } b = 0.0189 \quad C_2 = 6.38 \times 10^{-15}$$

$$\text{2nd minimum: } b = 0.0253 \quad C_2 = 8.25 \times 10^{-15}$$

$$\text{2nd maximum: } b = 0.0261 \quad C_2 = 8.38 \times 10^{-15}$$

These values yielded an average value for  $K$  of  $0.095 \pm .002$ . Thus it appeared that a value of  $K$  of 0.1 was a reasonable estimate of the ratio of scattering cell pressure to Baratron pressure.

Figure 19 shows the signal from the 50-50 mix with no microwave excitation (19a) and with about 110 watts of microwave power applied to the discharge (19b). The partial pressure of  $N_2$  in the scattering

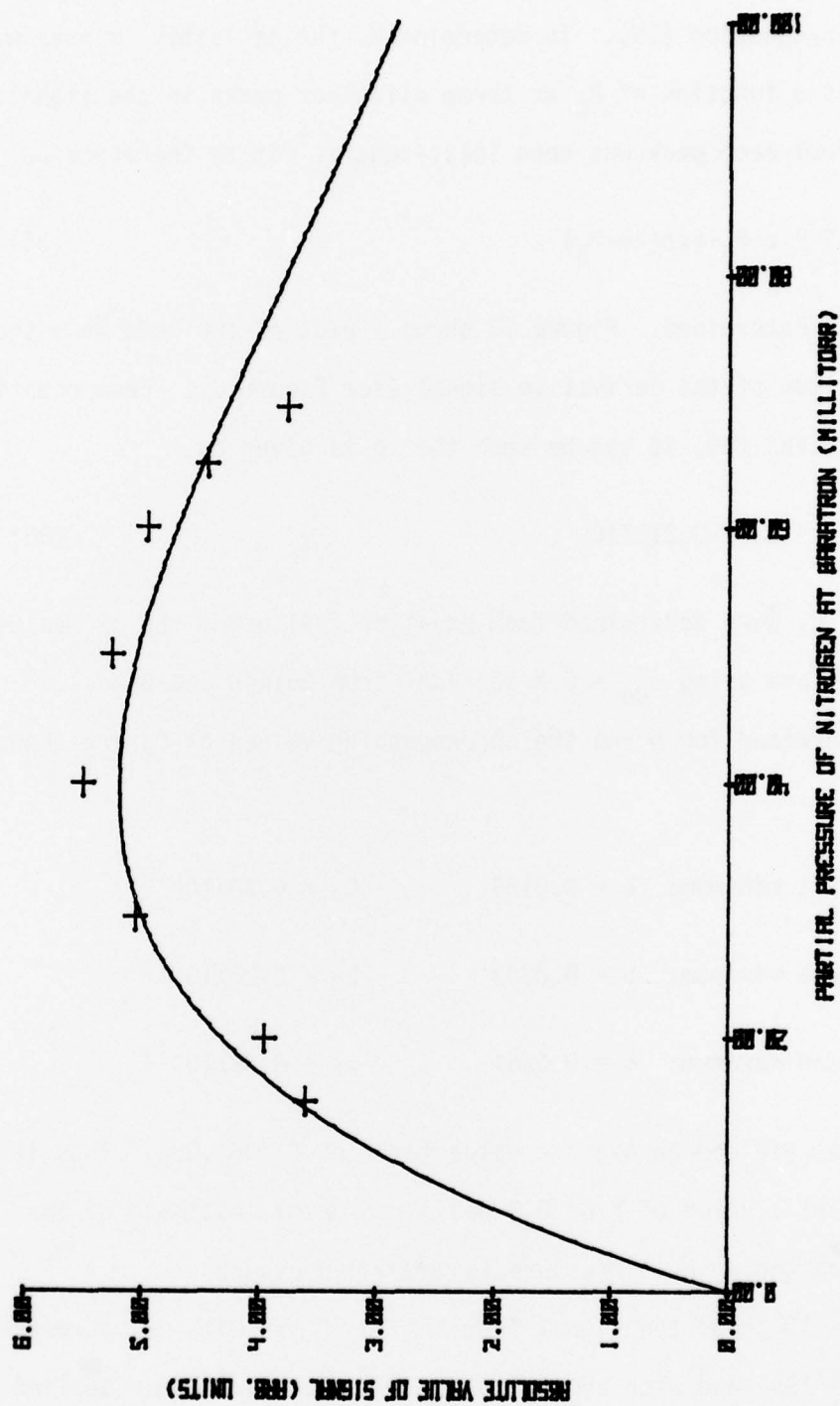
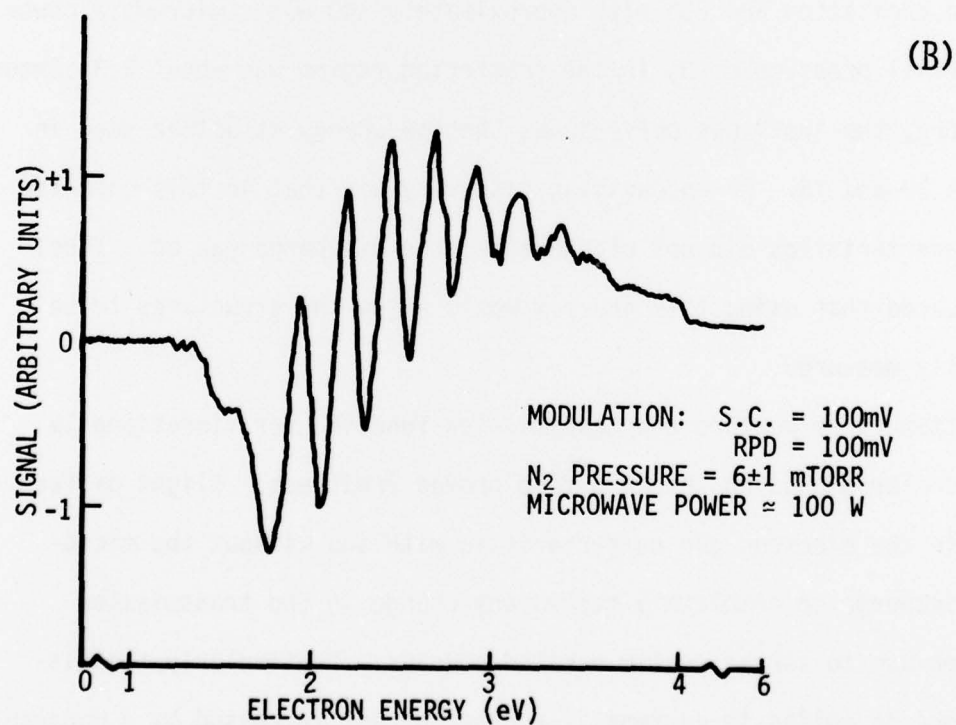
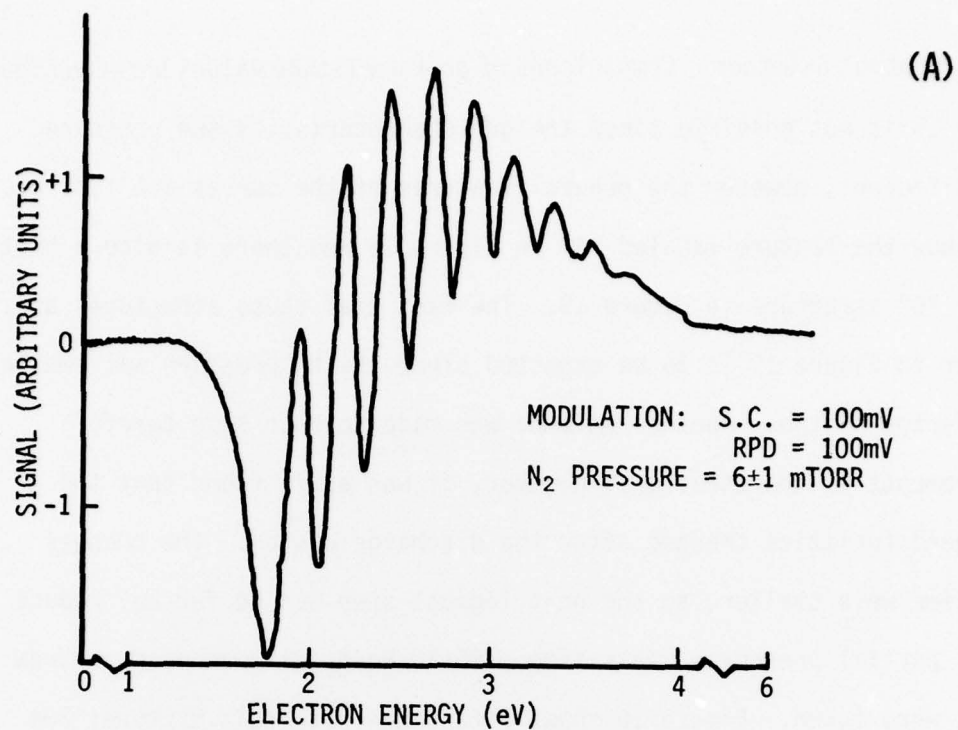


FIGURE 18 - PRESSURE DEPENDENCE OF SIGNAL FROM SECOND MINIMUM OF  $N_2$  DERIVATIVE



DERIVATIVE SIGNAL FROM "NORMAL" (A) AND  
"PRE-EXCITED" (B) 50-50 N<sub>2</sub>-HE MIX

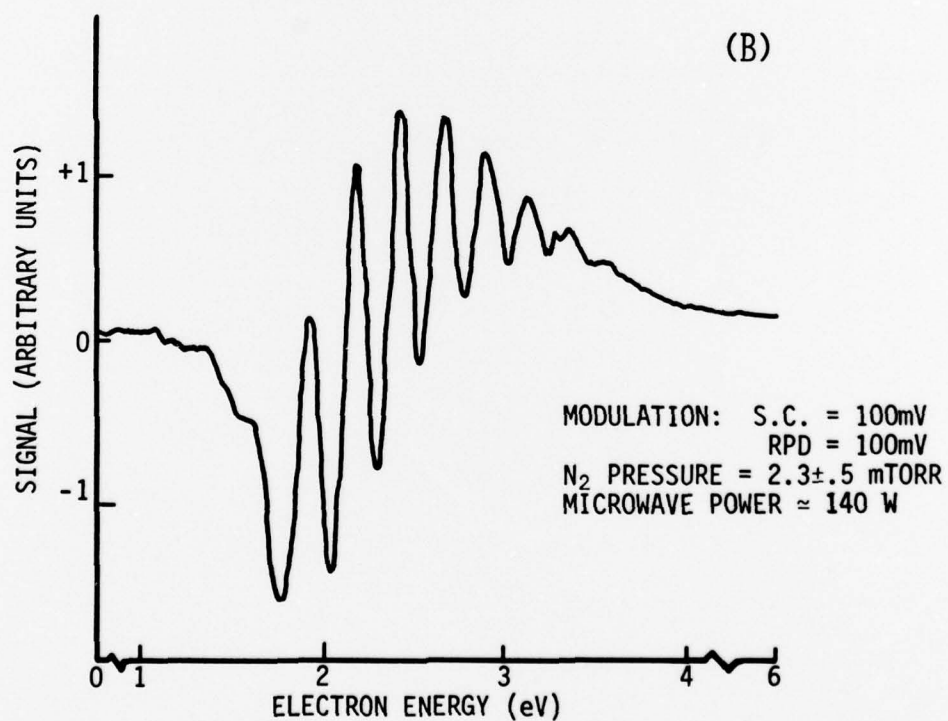
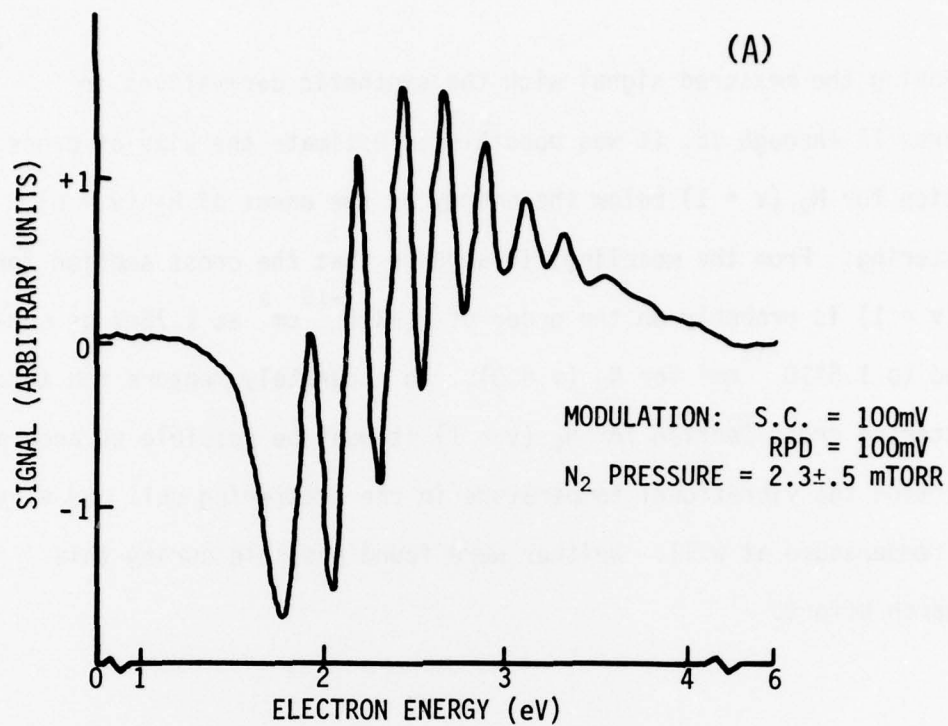
FIGURE 19



region is about  $6 \pm 1$  mtorr. Comparisons of peak amplitude values between Figures 16 and 19 is not possible since the gun characteristics and pressure were different, however the general features of the curves are similar. Both show the feature labeled "A" in Figure 16 and there is also a hint of the "B" structure in Figure 19. The fact that these structures are smaller in Figure 19 is to be expected since the  $N_2$  pressure was smaller by a factor of two. Another attempt was made to make some careful measurements of the structure; however, it was again found that the gun characteristics changed after the discharge was on. The changes this time were smaller, so the next logical step was to further reduce the  $N_2$  partial pressure. This time a 90-10 He- $N_2$  mix was used and new curves were taken. Figure 20 shows data taken with this mixture; 20a with no excitation and 20b with approximately 140 watts microwave power. The partial pressure of  $N_2$  in the scattering region was about  $2.3 \pm .5$  mtorr. As before, the "hot" gas curve shows the low energy structure seen in Figures 19 and 16. An encouraging discovery was that in this case the gun characteristics did not change after the discharge was on. Thus, it appeared that using this gas mix would allow the structures to be carefully measured.

Attempts to measure the transmission function for vibrationally excited nitrogen using the MRPD mode proved fruitless. Slight differences in the electron gun characteristic with and without the microwave discharge on completely masked any change in the transmission function due to vibrationally excited species. Particularly troublesome were dc shifts in current, i.e. the current increased by a constant value throughout the range. While these shifts did not grossly affect the derivative signal, they made MRPD measurements impossible. By





DERIVATIVE SIGNAL FROM "NORMAL" (A) AND  
"PRE-EXCITED" (B) 10-90 N<sub>2</sub>-He MIX

FIGURE 20

comparing the measured signal with the synthetic derivatives in Figures 12 through 15, it was possible to estimate the size of cross section for  $N_2$  ( $v = 1$ ) below the energy of the onset of  $N_2$  ( $v = 0$ ) scattering. From the modeling, it appears that the cross section for  $N_2$  ( $v = 1$ ) is probably on the order of  $2.5 \times 10^{-15} \text{ cm}^2$  at 1.75eV as compared to  $1.5 \times 10^{-15} \text{ cm}^2$  for  $N_2$  ( $v = 0$ ). To accurately measure the total scattering cross section for  $N_2$  ( $v = 1$ ) it must be possible to accurately determine the vibrational temperature in the scattering cell and vary the temperature at will. Neither were found possible during this research effort.

## REFERENCES

1. Michejda, J.A. and Burrow, P.D., "Observation of Vibrationally Excited Nitrogen with a Simplified Electron Transmission Apparatus", J. Appl. Phys., 47, 2780 (1976).
2. Dixon, A.J., Harrison, M.F.A. and Smith, A.C.H., "A Measurement of the Electron Impact Ionization Cross Section of Helium Atoms in Metastable States", J. Phys. B: Atom. Molec. Phys., 9, 2617 (1976).
3. Hall, R.I. and Trajmar, S., "Scattering of 4.5 eV Electrons by Ground State and Metastable Oxygen Molecules", J. Phys. B: Atom. Molec. Phys., 8, L293 (1975).
4. Burrow, P.D. and Michejda, J.A., "Detection of Vibrationally Excited Nitrogen by Electron Transmission", IX International Conference on the Physics of Electronic and Atomic Collisions (Univ. of Wash. Press, Seattle, 1975) p.949.
5. Schulz, G.J., "Resonances in Electron Impact on Atoms", Rev. Mod. Phys., 45, 378 (1973).
6. Kerwin, L., Marmet, P. and Carete, J.D., in Case Studies in Atomic Collision Physics I (ed. by McDaniel, E.W. and McDowell, M.R.C.), North-Holland Publishing Company, Amsterdam London (1969), chap. 9.
7. Schultz, G.J., "Resonances in Electron Impact on Diatomic Molecules", Rev. Mod. Phys., 45, 423 (1973).
8. Burrow, P.D., Michejda, J.A., and Jordon, K.D., "Resonances in Electron Scattering From Hydrocarbon Molecules", 29th Annual Gaseous Electronics Conference (Cleveland, Ohio, 1976), abstract L3.
9. Sanche, L. and Schulz, G.J., "Electron Transmission Spectroscopy: Resonances in Triatomic Molecules and Hydrocarbons", J. Chem. Phys., 58, 479 (1973).
10. Golden, D.E., "Analysis of the Sensitivity of Low Energy Electron Transmission Experiments", Rev. Sci. Instrum., 44, 1339 (1973).
11. Golden, D.E., Koepnich, N.G., and Fornari, L., "Comparison of Modulated Retarding Potential Difference and Retarded Energy Modulated Electron Spectrometers", Rev. Sci. Instrum., 43, 1249 (1972).
12. Taylor, John R. Scattering Theory: The Quantum Theory on Non-Relativistic Collisions (John Wiley and Sons, New York 1972), Chap. 13.
13. Burke, P.G., "Resonances in Electron Scattering and Photon Absorption", Adv. Phys., 14, 521 (1965).

14. Smith, K., "Resonant Scattering of Electrons By Atomic Systems", Rep. Prog. Phys., 29, 373 (1966).
15. Bardsley, J.N. and Mandal, F., "Resonant Scattering of Electrons by Molecules", Rep. Prog. Phys., 31, 472 (1968)
16. Taylor, H.S., "Models, Interpretations, and Calculations Concerning Resonant Electron Scattering Processes in Atoms and Molecules", Adv. Chem. Phys., 18, 91 (1970)
17. Schulz, G.J., in Principles of Laser-Plasmas (ed. by George Bekefi, Wiley-Interscience, New York, 1976) chp. 2.
18. Actually, Taylor<sup>16</sup> classifies the resonances into three groups, however Taylor's C.E.II group and third group are combined into the group called Type II in this work.
19. Birtwistle, D.T. and Herzenberg, A., "Vibrational Excitation of N<sub>2</sub> by Resonance Scattering of Electrons", J. Phys. B: Atom. Molec. Phys., 4, 53 (1971).
20. Chandra, N. and Temkin, A., "Hybrid Theory and Calculation of e-N<sub>2</sub> Scattering", Phys. Rev. A., 13, 188 (1976)
21. Golden, D.E., "Low-Energy Resonance in e<sup>-</sup>-N<sub>2</sub> Total Scattering Cross Sections: The Temporary Formation of N<sub>2</sub><sup>-</sup>", Phys. Rev. Lett., 17, 847 (1966).
22. Golden, D.E. and Zecca, A., "An Energy Modulated High Energy Resolution Electron Spectrometer", Rev. Sci. Instrum., 42, 210 (1971).
23. Schöwengerdt, F.D. and Golden, D.E., "A Double-Modulation Technique for Obtaining High-Resolution Energy-Differentiated Electron Transmission Spectra", Rev. Sci. Instrum., 45, 391 (1974).
24. Fehsenfeld, F.C., Evenson, K.M., and Broida, H.P., "Microwave Discharge Cavities Operating at 2450 MHz", Rev. Sci. Instrum., 36, 295 (1965).
25. McCarroll, B., "An Improved Microwave Discharge Cavity for 2450 MHz", Rev. Sci. Instrum., 41, 279 (1970).
26. Van Atta, C.M., Vacuum Science and Engineering, McGraw-Hill, Inc. (1965), Chp.2.
27. Schmeltekopf, A.L., Fehsenfeld, F.C., Gilman, G.I., and Ferguson, E.E., "Reaction of Atomic Oxygen Ions With Vibrationally Excited Nitrogen Molecules", Planet Space Sci., 15, 401 (1967).
28. Starr, W.L., "Excitation of Electronic Levels of Sodium by Vibrationally Excited Nitrogen", J. Chem. Phys., 43, 73 (1965).



29. Young, S.J. and Horn, K.P., "Measurements of Temperatures of Vibrationally Excited  $N_2$ ", J. Chem. Phys., 57, 4835 (1972).
30. Bray, K.N.C., "Vibrational Relaxation of Anharmonic Oscillator Molecules: Relaxation under Isothermal Conditions", J. Phys. B. (Proc. Phys. Soc.), 1, 705 (1968).
31. Black, G., Wise, H., Schter, S., and Sharpless, R., "Deexcitation of Metastables at Plasma Boundaries", SRI Project PYU-1959 Final Report to ARL, ARL 73-0182 (1973).
32. Herzberg, G. Molecular Spectra and Molecular Structure. I. Spectra of Diatomic Molecules, 2nd edition, Van Nos Reinhold Co. (1950).
33. See for example: Wylie, C.R., Jr., Advanced Engineering Mathematics, 3rd edition, McGraw-Hill Book Company (1966), chp. 9.
34. See for example: Gerald, C.F., Applied Numerical Analysis, Addison-Wesley Publishing Company (1970), chp. 1.
35. See for example: Levich, B.G., Theoretical Physics Volume 3 - Quantum Mechanics, North Holland Publishing Company (1973), chp. 11, p. 399.
36. Kieffer, L.J., A Compilation of Electron Collision Cross Section Data for Modeling Gas Discharge Lasers, JILA Information Center Report 13, Boulder (1973).
37. Garscadden, A., private communication, 1975.
38. Golden, D.E. and Bandel, H.W., "Absolute Total Electron-Helium-Atom Scattering Cross Sections for Low Electron Energies", Phys. Rev., 138, A14 (1965).